International Journal of
Molecular Sciences

MDPI

Review

BODIPYs in PDT: A Journey through the Most Interesting Molecules Produced in the Last 10 Years

Miryam Chiara Malacarne, Marzia Bruna Gariboldi and Enrico Caruso *

Department of Biotechnology and Life Sciences (DBSV), University of Insubria, Via J.H. Dunant 3, 21100 Varese, Italy
* Correspondence: enrico.caruso@uninsubria.it; Tel.: +39-0332421541

Abstract: Over the past 30 years, photodynamic therapy (PDT) has shown great development. In the clinical setting the few approved molecules belong almost exclusively to the porphyrin family; but in the scientific field, in recent years many researchers have been interested in other families of photosensitizers, among which BODIPY has shown particular interest. BODIPY is the acronym for 4,4-difluoro-4-bora-3a, 4a-diaza-s-indacene, and is a family of molecules well-known for their properties in the field of imaging. In order for these molecules to be used in PDT, a structural modification is necessary which involves the introduction of heavy atoms, such as bromine and iodine, in the beta positions of the pyrrole ring; this change favors the intersystem crossing, and increases the $^1O_2$ yield. This mini review focused on a series of structural changes made to BODIPYs to further increase $^1O_2$ production and bioavailability by improving cell targeting or photoactivity efficiency.

Keywords: 4,4-difluoro-4-bora-3a,4a-diaza-s-indacene; BODIPY; photodynamic therapy; photosensitizer

Citation: Malacarne, M.C.; Gariboldi, M.B.; Caruso, E. BODIPYs in PDT: A Journey through the Most Interesting Molecules Produced in the Last 10 Years. *Int. J. Mol. Sci.* **2022**, *23*, 10198. https://doi.org/10.3390/ijms231710198

Academic Editor: Christian Celia

Received: 25 August 2022
Accepted: 31 August 2022
Published: 5 September 2022

1. Introduction

1.1. Photodynamic Therapy (PDT)

Photodynamic therapy (PDT) [1,2] is an innovative technique that combines three components which are individually harmless but which when combined cause damage to nearby biomolecules (Figure 1).

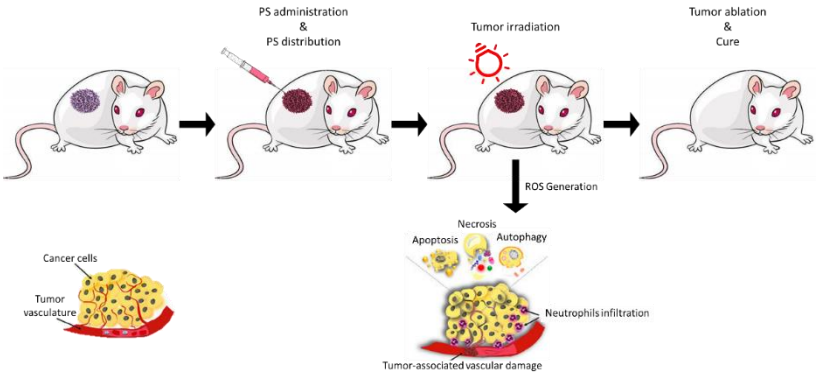

Figure 1. Schematic PDT Treatment: photodynamic strategy involves photosensitizer (PS) administration (local or systemic injection). Light irradiation is applied depending on the drug-light interval (time necessary to drug accumulation within the tumor). The activation of PS leads to the generation of $^1O_2$ and ROS that cause cancer cell death through apoptosis, necrosis or autophagy.

Nowadays, PDT is used for diverse pathologies, and it is gaining interest in cancer treatment [2–8]. PDT involves three components: a photosensitizer (PS), a molecule that has a high degree of unsaturation that is able to capture the energy provided by the second component, light at an appropriate wavelength; this energy is then transferred to the third

component, molecular oxygen [1,9,10]. Specifically, once irradiated, the PS in the excited electronic state is highly unstable and will therefore tend to return to the ground state. The return to the ground state can occur through the emission of fluorescence, an excellent property in the clinical setting for imaging or photodetection, and/or heat [11]. Alternatively, and based on physico-chemical characteristics, the PS can undergo an intersystem crossing (ISC); with this step the PS will go into a more stable triplet state (^{3}PS*) with an inverted spin of an electron. ^{3}PS* can return to the ground state by emitting phosphorescence or it can interact with molecular oxygen (O_2) [12] thus leading to the formation of singlet oxygen ($^1O_2$) in what is called a Type II reaction [13–15]. Type I reactions can also occur; in this case the PS interacts directly with a substrate [16–20], such as the cell membrane or a molecule, thus transferring a proton or an electron to the substrate to form radicals which will then react with O_2 to form the superoxide anion ($O_2^{\bullet -}$), the hydroxyl radical ($OH^{\bullet}$) and hydrogen peroxide (H_2O_2) [6,21–24]. Type I and Type II reactions can occur simultaneously, even though photoreaction of type II is predominant [13,25,26]. ROS that are generated by type I and II reactions are mainly responsible for PDT-induced cell death [27,28]. These species are extremely toxic and, once formed, can strongly reduce malignant cells through necrosis, apoptosis, autophagy [4,10,29–31], and, as reported by many authors, can cause inflammatory/immune responses [32–38].

One of the three crucial elements of PDT is the PS [39]. PSs used are generally colored substances that share, as a common feature, an extensive electronic conjugation by a high number of conjugated double bonds to allow the interaction of π electrons with low energy radiations such as visible light.

The ideal PS for therapeutic application should have a selective accumulation in the tumor tissue [11]. The accumulation is favored by a certain degree of lipophilicity which favors cellular uptake but at the same time is also favored by a certain degree of hydrophilicity which facilitates its administration; the two concepts can be exemplified with the term amphiphilia [7,11,39]. PS must also have no or negligible intrinsic toxicity to preserve healthy tissues [6,39]. From a chemical point of view, PS should be easily synthesized in pure formulation, have a high molar extinction coefficient [7] and a high quantum yield of $^1O_2$ [40]. The ideal PS should be activated at wavelengths of between 680 and 800 nm for a deeper penetration of the light [41].

Over the years various generations of PSs have been obtained to meet all the requirements of the ideal PS. Historically, the PSs are divided into first, second and third generation [1,11,42].

The first generation includes naturally derived PSs belonging to the porphyrin family that were developed in the 1970s and early 1980s. The first preparations for use in PDT were based on a fairly complex mixture of Hematoporphyrin-derived (HpD) porphyrins [1,43]. HpDs showed better tissue selectivity for tumors and less photosensitizing potential of the skin [44,45], but they have limitations such as low chemical purity, poor tissue penetration and skin hypersensitivity to light [1,39,46–48].

In the 1980s, to overcome those limitations, several hundreds of substances with potential for photosensitizing had been proposed, however, only a few were used in clinical trials. The second generation includes synthetic PSs such as 5-aminolevulinic acid, benzoporphyrin derivatives, texaphyrins, chlorins, bacteriochlorins, BODIPYs, anthraquinones, xanthenes, cyanines and curcuminoids [1,5,39,49–53]. Those compounds show higher chemical purity, a higher yield of $^1O_2$ formation and better penetration [6]. The strong limitation turns out to be water solubility.

Using second generation PSs as a basis and binding them with cargos to allow targeted accumulation in the tumor site, the third generation of PSs was obtained [10,54]. In this category PSs are conjugated with organic and inorganic polymers, nanoparticles, liposomes, monoclonal antibodies, antibody fragments, protein/peptides (such as transferrin, EGF, somatostatin and insulin), carbohydrates, folic acid, and many others [1,24,55,56]. These modifications lead to enhance targeting and absorption of the PS in tumoral and drained-vasculature cells within the tumors [57]. Many PSs belonging to this generation are currently under development or undergoing clinical trial.

1.2. BODIPYs

The first member of 4,4-difluoro-4-bora-3a,4a-diaza-s-indacene dyes (hereafter abbreviated to BODIPYs) was reported by Treibs and Kreuzer in 1968 [58] although relatively little attention was given to their discovery until the end of the 1980s [59]. The potentials of this dyes for biological labeling and in many other science fields was later recognized and a series of study brought attention on them.

In addition to the high fluorescence emission (Φ), the BODIPYs are characterized by a high molar extinction coefficient (ε) in the visible region, limited changes by environmental conditions (e.g., polarity of the solvent or pH) [60], by a high lipophilicity [61] and a good resistance to photobleaching (the phenomenon of chemical destruction of a fluorophore by light [62]).

The absorption and emission characteristics of the BODIPY can be adjusted by adding suitable substituents on the main structure of the BODIPY itself. The effect is particularly evident when the substituent is bonded to one of the carbon atoms of a pyrrole ring [63]. On the contrary, the presence of an aromatic group in position 8 (meso) exerts a very weak effect, mainly explained by the weak electronic interaction between the aromatic ring and the main structure of the BODIPY [55].

Any structural difference on the *meso*-aryl group does not greatly affect the intensity and wavelength of the absorption and fluorescence bands, however the degree of polarity of this part can modulate the degree of amphiphilicity of the molecule.

The presence of substituents in positions 2 and 6 of pyrrole (β positions) involves some evident effects; for example, the presence of alkyl groups or heavy atoms has direct repercussions on the energy of the HOMO and LUMO orbitals and on the triplet state so as to influence the absorption and emission phenomena of UV-Vis radiation [64,65].

In addition to the well-known fluorescence that makes these molecules excellent biomarkers, a new important application field of BODIPYs concerns photodynamic therapy (PDT) as they can be used as photosensitizers (PS), after appropriate modifications [61].

A fundamental modification to increase the probability of ISC and the quantum yield of $^1O_2$ formation is the introduction in some specific positions of a heavy atom, such as iodine or bromine. A heavy atom can quench the fluorescence and facilitate the transition to triplet state. Heavy atoms either in solution (external Heavy Atom Quenching HAQ) or incorporated in the molecule (internal HAQ) assumed to quench fluorescence by perturbating S1 state via spin orbit interactions that modifies electron's atomic energy levels. The transition between the T_1 state and ground state are forbidden due to the spin changes, this results in a relatively long-lived and reactive excited configuration that can interact with other molecule forming complexes or radicals [40,56,61,65].

Iodine seems to severely quench fluorescence, suggesting that the intersystem crossing efficiency (Φ_{ISC}) has been enhanced by the internal heavy atom effects. Interestingly 2I-BODIPYs showed a narrow peak in NIR spectrum that is characteristic of $^1O_2$ generating molecules [40,66–71]. The incorporation of more heavy atoms in BODIPY core does not effectively enhance the $^1O_2$ quantum yield; on the contrary it appears to increase dark toxicity.

2. BODIPYs Studies

Substituents are generally attached in positions 4 (boron center); 3,5 (α-positions); 1,2,6,7 (*β*-positions), and 8 (*meso* position). In this context, we will show new structural derivatives of BODIPY core and their strategy to improve delivery and efficiency [56,59,66]. Principal modifications are the addition of groups that modify chemical and physical properties (hydrophilicity, absorption wavelength, ISC efficiency, etc.), or improve the interaction with biological medium (environment-response, association with targeting molecules, etc.) [56,59,66,72].

Modifications to their structures enable the tuning of their fluorescence characteristics, enhancing their capacity for $^1O_2$ generation. The stability of the core structure and its tendency to maintain photochemical properties even with complex groups as substituents in some positions makes BODIPYs an interesting class of compounds for PDT [56,59,72].

2.1. Structure-Activity

One of the important aspects in the study of the various PSs is to evaluate the relationship that exists between the chemical structure and the photodynamic activity of the PS; in fact, this could allow the design of targeted syntheses. In recent years many authors have tried to analyze this type of relationship in various series of PS such as porphyrins [73,74], the pyropheophorbides [75] and phthalocyanines [76].

Even in the case of BODIPYs this type of approach is extremely important for their application in PDT [40,71,77–85].

Recently, we characterized a panel of twenty-four new BODIPYs all united by an aromatic ring in *meso* position and by the presence of iodine atoms in *β*-positions [86]. The panel shows different atoms or groups as substituents of the aromatic ring. All compounds were characterized from a physico-chemical point of view (generation of $^1O_2$, fluorescence and lipophilicity) and for their activity on the human ovarian carcinoma cells SKOV3. A quantitative structure-activity relationship (QSAR) analysis was also performed to understand how the substituent could affect PS activity.

Data obtained demonstrate that the presence of an aromatic ring is essential to obtain a high production of $^1O_2$ and high phototoxicity of the compounds. Of the twenty-four compounds analyzed, two showed high activity (compounds **2** and **8**).

The first is characterized by the presence of a methoxy group in the *para* position while the other has two chlorine atoms in the *ortho* and *ortho'* position (Figure 2). The differences in regioisomerism and in the electronic effect confirm the absence of correlations between the substituents and the efficacy of the photo-induced action.

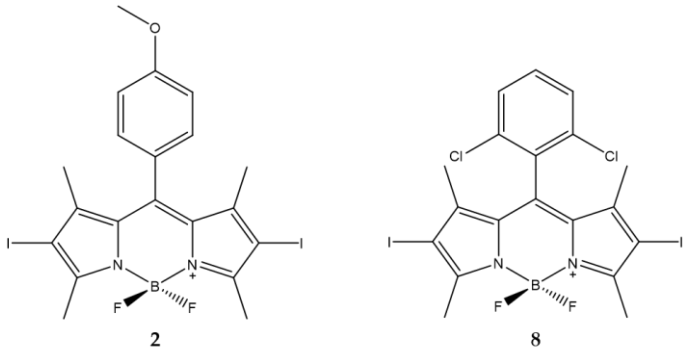

Figure 2. Chemical structures of compounds **2** and **8** [86].

The presence of iodine atoms in the *β*-positions of the pyrrole determine a high production of $^1O_2$. The IC_{50} were in the range of 1-2 nM for the BODIPY derivatives with the exception of compounds **2** and **8** (Table 1).

Table 1. Physico-chemical properties and biological data obtained for compounds **2** and **8** [86].

	2	**8**
λ_{abs} [a]	534 nm	548 nm
ε	61,500 $M^{-1}cm^{-1}$	76,400 $M^{-1}cm^{-1}$
Φ_{fluo} [b]	0.02	0.02
$^1O_2$ QY [c]	1.04	1.53
$IC_{50\ (SKOV3)}$ [d]	0.65 nM	0.77 nM

[a] 10 µM solution in Dichloromethane (DCM). [b] In DCM with fluorescein (0.1 M NaOH, 0.85) as standard. [c] In isopropanol with DPBF (1,3-diphenylisobenzofuran) as indicator and Rose Bengala as standard. [d] 2 h of irradiation with a green LED device (fluence rate 25.2 J/cm^2).

Based on these results, the effect of chains of different length on the hydroxyl groups was evaluated. Two BODIPYs with the presence of hydro-carbon chains of different lengths placed in position 4 (*para*) of the phenyl ring placed in *meso* position of the core were analyzed [87]. Specifically, compounds **3** and **4** (Figure 3) have carbon chains consisting of four and eight atoms, respectively, to obtain a different degree of lipophilicity of the two molecules. This difference should make it possible to establish a correlation between the length of the alkyl chain and the photodynamic activity. A bromine atom was presented at the end of each chain to make these molecules more versatile and eventually allow the bond with nanoparticles [88].

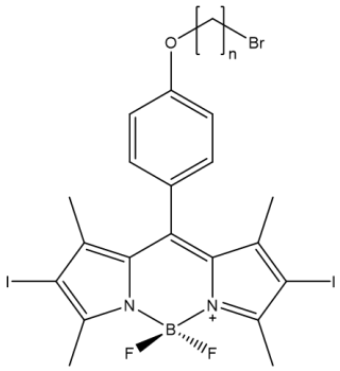

3 n=4
4 n=8

Figure 3. Chemical structures of compounds **3** and **4** [87].

The analyzes carried out confirmed that the presence of alkyl chains of different lengths affects the degree of lipophilicity and consequently also the photodynamic effect. Compound **3** has a fair degree of lipophilicity associated with an effective photodynamic action on tumor cells; on the contrary, the more lipophilic compound **4** has a lower photodynamic activity probably due to the formation of aggregates in aqueous medium (Table 2).

Table 2. Physico-chemical properties and biological data obtained for compounds **3** and **4** [87].

	3	**4**
λ_{abs} [a]	533 nm	534 nm
ε	66,072 $M^{-1}cm^{-1}$	41,500 $M^{-1}cm^{-1}$
λ_{em} [a]	553 nm	554 nm
Φ_{fluo} [b]	0.01	0.01
$^1O_2$ QY [c]	1.10	1.11
$IC_{50\ (HCT116)}$ [d]	2.0 nM	11.7 nM
$IC_{50\ (SKOV3)}$ [d]	3.56 nM	15.61 nM
$IC_{50\ (MCF7)}$ [d]	6.88 nM	23.11 nM

[a] 10 µM solution in DCM. [b] In DCM with fluorescein (0.1 M NaOH, 0.85) as standard. [c] In isopropanol with DPBF as indicator and Rose Bengala as standard. [d] 2 h of irradiation with a green LED device (fluence rate 25.2 J/cm^2).

As already highlighted the main problem with these PSs leads to their solubility in aqueous medium. Belfield et al. designed a BODIPY decorated in meso position with a polyethylene glycol chain to enhance solubility and to prevent aggregation in aqueous solution [89].

Compound **3** (Figure 4) was characterized as regards absorption, fluorescence and $^1O_2$ production. The ability to produce $^1O_2$ was evaluated by direct measurement of near infrared luminescence. The quantum yield of $^1O_2$ generation is higher than that of the standard used as a control (0.93 for **3**, 0.82 for acridine used as control). IC_{50} were estimated at 10 μM against Lewis lung carcinoma cells pre-treated with compound **3** and exposed to a light dose of 3.5 mW/cm^2 (Table 3).

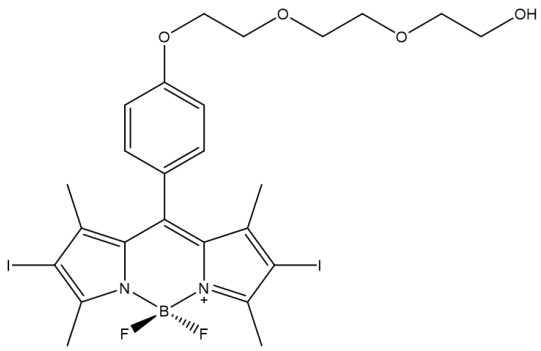

3

Figure 4. Chemical structures of compound **3** [89].

Table 3. Physico-chemical properties and biological data obtained for compound **3** [89].

	3
λ_{abs} [a]	528 nm
ε	75,500 $M^{-1}cm^{-1}$
λ_{em} [a]	546 nm
Φ_{fluo} [b]	0.02
$^1O_2$ QY [c]	0.93
$IC_{50\ (LLC)}$ [d]	10.0 μM

[a] In acetonitrile. [b] Determined by a standard relative method with Rhodamine 6 G ($\Phi_{fluo} \approx 0.94$ in ethanol) as a reference. [c] In acetonitrile using acridine as standard. [d] Irradiation with a light dose of 3.5 mW/cm^2 from a filtered light source (522 ± 40 nm) for different time.

In addition, the cell death mechanisms induced following photodynamic treatment were evaluated and necrosis prevails over apoptosis process. The results obtained show how it is feasible to obtain a BODIPY with a higher degree of hydrophilicity with at the same time excellent characteristics for use in PDT.

2.2. Singlet Oxygen Generation

Critical factor for the activity of BODIPY is certainly the production of $^1O_2$. The generation of $^1O_2$ in solution requires a photosensitizer (PS) which is converted to the triplet excited state (intersystem crossing, ISC) upon irradiation. The triplet state PS transfers energy to molecular oxygen in a type II process to produce $^1O_2$. The heavy atom effect has been a useful chemical approach to improve ISC in several molecules including BODIPY chromophores.

Lincoln et al., and Durantini et al., investigated the different photostability and PS efficiency for PDT of two BODIPYs bearing an acetoxymethyl substituent in the *meso* position and bromine or iodine atoms in positions 2 and 6 of the scaffold [90,91].

The presence of the substituent acetoxymethyl in meso position improves the photostability of the PS. (Figure 5). It was also observed that the presence of iodine (**I_2BOAc**) or

bromine (**Br_2BOAc**) atoms in both β-positions affects the production level of $^1O_2$. The PS bearing the two bromine atoms produced a lower level of $^1O_2$ than that bearing the iodine atoms. The production of $^1O_2$ by the bromine compound conferred a slight improvement in stability mainly attributable to the lower amount of oxidant generated (Table 4).

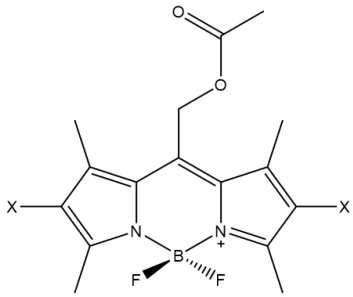

Br_2BOAc X=Br
I_2BOAc X=I

Figure 5. Chemical structures of compounds **Br_2BOAc** and **I_2BOAc** [90,91].

Table 4. Physico-chemical properties and biological data obtained for compounds **Br_2BOAc** and **I_2BOAc** [90,91].

	Br_2BOAc	**I_2BOAc**
λ_{abs} [a]	543 nm	550 nm
ε	81,000 $M^{-1}cm^{-1}$	96,000 $M^{-1}cm^{-1}$
λ_{em} [a]	562 nm	572 nm
Φ_{fluo} [b]	0.14	0.02
$^1O_2$ QY [c]	0.84	0.98
$IC_{50\ (HeLa)}$ [d]	140.0 nM	180.0 nM

[a] In acetonitrile. [b] Determined by the consumption of dimethylanthracene using Rose Bengal as a standard. [c] In acetonitrile using Rose Bengala as standard. [d] Irradiation with a 520 nm LED panel for 30 min.

Cytotoxicity studies conducted with the HeLa tumor cell line have shown that the compound bearing the bromine atoms is the most active. The localization of these compounds is mainly in the lipid membranes of the cell. Tests to evaluate the photodynamic activity of bacterial inactivation were carried out against Gram-negative *Escherichia coli*. The results obtained showed that both molecules are able to photo-kill *E. coli* already from a concentration of 5 µM, suggesting that both molecules have a PDT potential against *E. coli* and other Gram-negative strains.

A similar comparison between the two types of halogens bound in β-positions of the BODIPY was also carried out by Epelde-Elezcano et al., who studied the photo-physical properties of a series of BODIPYs bearing either two bromine atoms or two iodine in β-positions of the pyrrole of the BODIPY skeleton. Specifically, the measurement of $^1O_2$ production was carried out with an indirect assay using 9,10-dimethylanthracene (DMA) as a chemical probe and with a direct determination of the luminescence at 1276 nm of the $^1O_2$ with a NIR detector. The work demonstrates how the iodine atom favors the ISC over the bromine atom. In the same work the authors evaluate the impact of the *meso* substituent, observing how an electron donor substituent tends to decrease the production of $^1O_2$ compared to an analogous derivative bearing an electron withdrawing substituent. Furthermore, a strong decrease is observed in the case of electron donor substituents when there is free rotation of the substituent which favors the internal conversion process to the detriment of the ISC and therefore of the production of $^1O_2$ [92].

Turan et al., focused on synthesis of BODIPY derivatives that could be applied to enhanced fractional photodynamic therapy [93]. In this therapeutic strategy and to prevent photo-induced hypoxia, the light is administered intermittently (fractional PDT) to allow the replenishment of cellular oxygen with an increase in the time necessary for the effective

therapy. The study reported the synthesis of a BODIPY containing 2-pyridone (Figure 6) which in the dark conditions, through a thermal cycloreversion, becomes a source of $^1O_2$ [94–98].

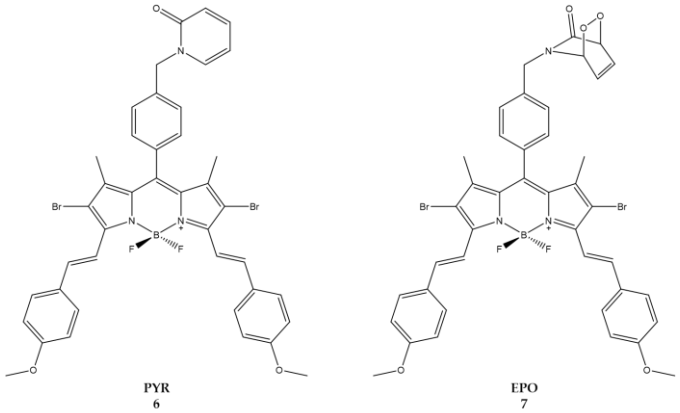

Figure 6. Chemical structures of compounds **6** (**PYR**) and **7** (**EPO**) [93].

When excited at a wavelength of 650 nm, molecule **6** (**Pyr**) generates $^1O_2$ which is partially stored in the form of 2-pyridone-endoperoxide (**7** or **EPO**). When irradiation is stopped **EPO** will undergo thermal cycloreversion to produce $^1O_2$ in the absence of light (Table 5) [99,100].

Table 5. Physico-chemical properties and biological data obtained for compounds **6** (**PYR**) and **7** (**EPO**) [93].

	6 (PYR)	**7 (EPO)**
λ_{abs} [a]	668 nm	667 nm
ε	22,200 $M^{-1}cm^{-1}$	74,200 $M^{-1}cm^{-1}$
λ_{em} [a]	697 nm	700 nm
Φ_{fluo} [b]	0.14	0.10
$^1O_2$ QY [c]	0.15	0.20
$IC_{50\ (HeLa)}$ [d]	49.0 nM	8.6 nM

[a] In DMSO. [b] In DMSO with Cresyl Violet ($\Phi_{fluo} \approx 0.66$ in methanol) as a reference. [c] In ethanol using Methylene blue as a reference ($^1O_2$ QY ≈ 0.52 in ethanol). [d] Irradiation cycles of light (λ = 655 nm, 10 min) and dark (50 min) with a total of 24 h of light exposure.

The molecules were tested against human cervical HeLa cells. Due to the low solubility, the compounds were prepared as micellar structures using the non-ionic surfactant cremophor EL [101]. IC_{50} was estimated at 8.6 nM and 49 nM for compound **7** and **6**, respectively. Results demonstrates how the continuous release of $^1O_2$ by the photosensitizer during the light-dark cycles has to be considered as a positive feature if we compare the cytotoxic effects with those of conventional photosensitizing agents.

Zou et al., instead focused on how the effect and configuration of the substituents of heavy atoms are important for $^1O_2$ generation [102]. A series of BODIPY derivatives was synthesized with one or two BODIPY units connected via a benzene ring; PSs thus obtained were then halogenated in *β*-positions with bromine or iodine atoms. The ability to produce $^1O_2$ and cytotoxic efficacy in HeLa cells was evaluated for each of the compounds.

The best producers of $^1O_2$ are compounds **4** and **6**, consisting of one and two units of iodinated BODIPY, respectively. Moreover, the insertion of two or more heavy atoms does not significantly affect the improvement of the $^1O_2$ produced (Table 6).

Table 6. Physico-chemical properties and biological data obtained for compounds **4** (**BDPI**) and **6** (**BBDPI**) [102].

	4 (BDPI)	6 (BBDPI)
λ_{abs} [a]	533 nm	540 nm
$^1O_2$ QY [b]	0.73	0.68
$IC_{50\ (HeLa)}$ [c]	1.0 μM	2.8 μM

[a] In DCM. [b] Using DPBF as the probe and methylene blue (ΦΔ = 0.57 in DCM) as standard. [c] Irradiation with a xenon lamp (40 mW/cm^2) for 8 min.

The synthesized compounds were then included in NPs to improve water solubility, required for cytotoxicity tests against HeLa cells. The MTT test showed that the most active compound is **6** (Figure 7). Given the good results obtained in vitro, compound **6** was also used for in vivo tests. In vivo, treatment with compound **6** led to a dramatic decrease in tumor growth and no tumor recurrence was observed. Biodistribution analysis showed that compound **6** accumulated in tumor cells and the liver. The selective irradiation of the tumor zone alone ensures that the liver is spared from possible photodynamic damage.

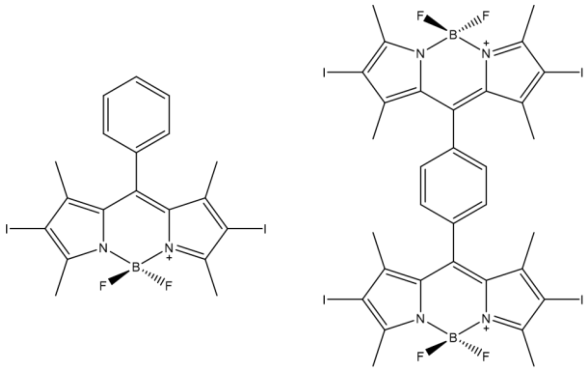

Figure 7. Chemical structures of compounds **4** (**BDPI**) and **6** (**BBDPI**) [102].

Pang et al., considered the dimerization of two BODIPYs to increase $^1O_2$ generation (Figure 8). In this case, the second BODIPY molecule is covalently linked in the beta position of the first BODIPY and can assume two positions, either orthogonal as in compounds **2b** and **2d** or angular (angle of about 30–40°) in compounds **2a** and **2c** [103].

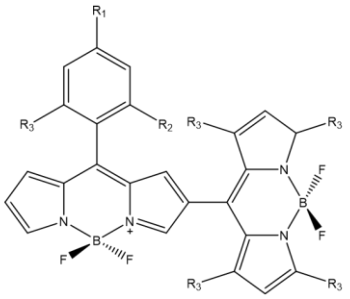

Figure 8. Chemical structures of compounds **2a**–**d** [103].

Following the synthesis, the authors took into consideration some spectroscopic properties and the $^1O_2$ production evaluated both through direct and indirect determination (Table 7).

Table 7. Physico-chemical properties and biological data obtained for compounds **2a**–**d** [103].

	2a	**2b**	**2c**	**2d**
λ_{abs} [a]	521 nm	507 nm	538 nm	507 nm
λ_{em} [a]	563 nm	540 nm	568 nm	542 nm
Φ_{fluo} [b]	0.007	0.002	0.002	0.002

[a] In DCM. [b] In DCM with fluorescein (0.1 M NaOH, 0.90) as standard.

The highest efficiency was observed for orthogonal meso–b linked dimer which confirm the data that Cakmak et al., had previously reported as well [101].

2.3. Uptake and Targeting

As reported by many authors [104–111], the aspect of cellular uptake and targeting has always been a very important aspect for all families of photosensitizers. Trying to increase cellular uptake as well as to make cellular penetration selective between healthy and tumor tissues is of primary importance, consequently cellular uptake and targeting are fundamental and interrelated factors.

2.3.1. Uptake

Shivran et al., synthesized three water soluble glucose conjugated BODIPYs and subsequently tested them on human lung cancer A549 cells. Of the three compounds, compound **4** features a glycosylated styryl appendix in position C-3 (Figure 9) [68]. The choice to insert a glucose on the PS is linked to the greater ability of the cancer cells to accumulate sugars.

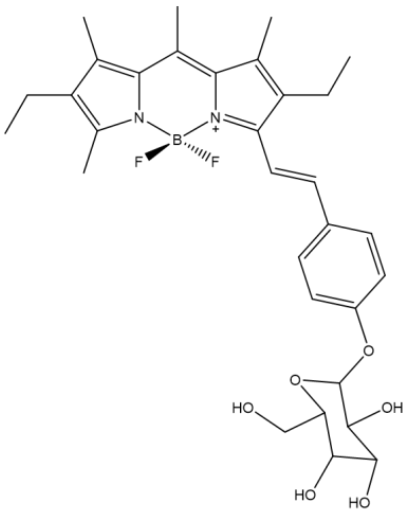

4

Figure 9. Chemical structures of compound **4** [68].

The emission spectrum of this compound is typical of a BODIPY with a high molar extinction coefficient and a high fluorescence emission. The introduction of the styryl group determines a bathochromic shift both in the absorption and in the maximum emission with respect to the BODIPY in which this group is absent. The IC_{50} value of all the compounds was evaluated and compound **4** is endowed with the greatest cytotoxicity (Table 8).

Table 8. Physico-chemical properties and biological data obtained for compound **4** [68].

	4
λ_{abs} [a]	573.8 nm
ε	8,2000 $M^{-1}cm^{-1}$
λ_{em} [a]	590 nm
Φ_{fluo} [b]	0.6
$IC_{50\ (A549)}$ [c]	2.7 µM

[a] In ethanol. [b] Relative to that of rhodamine 101 (Φ_{fluo} = 1.0 in EtOH). [c] Irradiation for 80 min (irradiance: 0.77 mW/cm^2).

Moreover, compound **4** accumulated rapidly in tumor cells. In addition, cell exposure to compound **4** led to apoptosis which is the prevailing cell death mechanism. Overall, the work in question demonstrated how it is possible to obtain a compound capable of having a selective capacity towards cancer cells in an economical and fast way.

Kuong Mai et al. [112] synthesized a water soluble BODIPY starting with a halogenated alkyl azide BODIPY to which a lactose motif is linked through an easy and straightforward CuAAC Click reaction [113]. The coupling of the lactose motif causes the compound to be soluble in water (Figure 10).

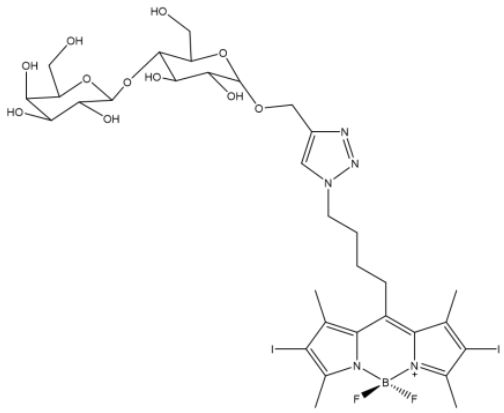

BDILa

Figure 10. Chemical structures of compound **BDILa** [112].

The emission and absorption spectra are consistent with those of the BODIPY family and the production of $^1O_2$ is high. The photodynamic activity of the PS was evaluated on three different tumor cell lines: human hepatoma Huh7, cervical cancer HeLa and breast cancer MCF7 and IC_{50} ranging from 0.6 to 0.5 µM (Table 9).

Table 9. Physico-chemical properties and biological data obtained for compound **BDILa** [112].

	BDILa
λ_{abs} [a]	526 nm
ε	41,800 $M^{-1}cm^{-1}$
λ_{em} [a]	542 nm
Φ_{fluo} [b]	0.02
$^1O_2$ QY [c]	0.47
$IC_{50\ (HeLa)}$ [d]	0.55 µM
$IC_{50\ (MCF7)}$ [d]	0.61 µM
$IC_{50\ (Huh7)}$ [d]	0.50 µM

[a] In H_2O. [b] In methanol. [c] In ethanol. [d] Irradiation for 20 min with a green LED (λ = 530 nm).

However, cell uptake was low, whatever the cell line tested, probably due to the presence of iodine atoms on the core of the BODIPY.

2.3.2. Targeting

Active targeted therapy of cancer refers to targeting the surface molecules on cancer cells using a small molecule to deliver cargo for therapeutic or diagnostic purposes. The cargo can be a cytotoxic drug, an imaging probe, or a photosensitizer [114].

Lysosomal Targeting

In 2019 Wang et al., obtained a BODIPY able to specifically targeting lysosomes [115]. The molecule obtained (**BDPI-Lyso**) has iodine atoms to generate $^1O_2$ and morpholine for targeting specifically the lysosomes (Figure 11) [116–118].

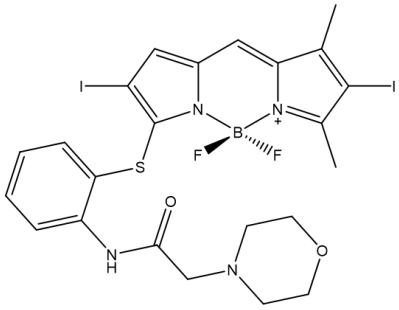

BDPI-Lyso

Figure 11. Chemical structures of compound **BDPI-Lyso** [115].

Physico-chemical analyzes showed that the absorption and fluorescence of the compound are slightly greater than that of the common BODIPYs due to the modification of the sulfur heteroatom. Moreover, under irradiation, the derivative produced higher level of $^1O_2$ in acidic versus physiological pH (Table 10).

Table 10. Physico-chemical properties and biological data obtained for compound **BDPI-Lyso** [115].

	BDPI-Lyso
λ_{abs} [a]	545 nm
ε	41,900 $M^{-1}cm^{-1}$
λ_{em} [a]	572 nm
Φ_{fluo} [a]	0.05
$^1O_2$ QY [a]	0.95
$^1O_2$ $QY_{pH=5}$ [b]	0.51
$^1O_2$ $QY_{pH=7}$ [c]	0.38
$IC_{50\ (Bel\text{-}7402)}$ [d]	0.4 μM

[a] In ethanol. [b] In ethanol/PBS = 1:1, pH = 5.10. [c] In ethanol/PBS = 1:1, pH = 7.24. [d] Irradiation for 30 min with green light (λ = 555 nm, light dose: 4 mW/cm^2).

This leads to the assumption that BODIPY exhibits greater photo-toxic effects in acid compartments such as lysosomes than in neutral organelles. In fact, the BODIPY derivative was localized in lysosomes as demonstrated by cell imaging performed with hepatoma Bel-7402 cells. Moreover, IC_{50} was estimated at 0.4 μM after cell pretreatment with the molecule and light exposition for 30 min duration.

Similarly, Li et al. [119] synthetized a BODIPY (**MBDP**) (Figure 12) containing morpholine for lysosomal targeting and iodine atoms on the BODIPY core to produce $^1O_2$. Triethylene glycol monomethyl ether benzaldehyde was added through the condensation of Knoevenagel to obtain the desired compound [120].

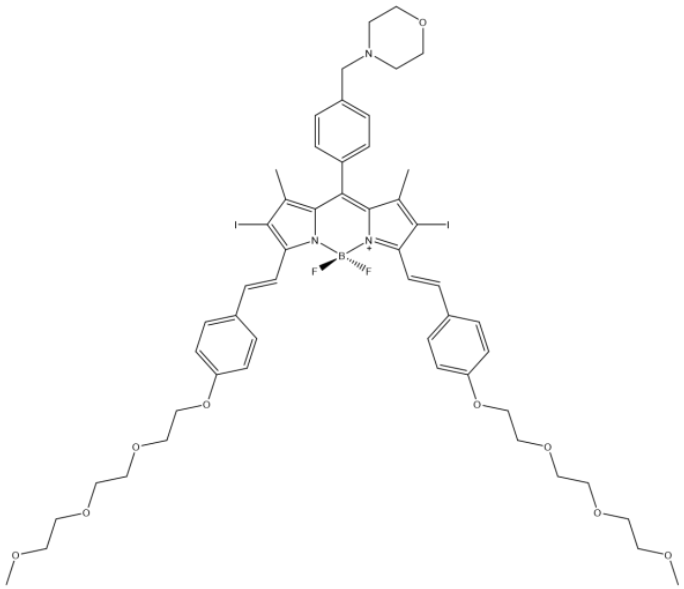

Figure 12. Chemical structures of compound **MBDP** [119].

The analysis of the absorption spectrum of the compound showed that there is an intense cui bands at 660 nm. At 660 nm, the compound under LED light produces high levels of $^1O_2$ (Table 11).

Table 11. Physico-chemical properties and biological data obtained for compound **MBDP** [119].

	MBDP
λ_{abs} [a]	660 nm
ε	83,226 $M^{-1}cm^{-1}$
λ_{em} [a]	694 nm
Φ_{fluo} [b]	0.11
$^1O_2$ QY [c]	0.64
$IC_{50\ (MCF7)}$ [d]	0.2 µM

[a] In DCM. [b] In DCM with Cresyl Violet (Φfluo ≈ 0.66 in methanol) as a reference. [c] Using DPBF as the $^1O_2$ capture agent and methylene blue as standard (Φ = 0.57 in DCM). [d] Irradiation with 660 nm LED red light (20 mW/cm^2, 48 J/cm^2).

Cytotoxicity tests were performed on the MCF7 cell line with an estimated IC_{50} at 0.2 µM. The colocalization experiments confirmed the effective lysosomal localization of the compound. It was also possible to determine how, following irradiation, the lysosomes containing photosensitizer break down following $^1O_2$ and ROS generation. In addition, the BODIPY derivative could also be used for NIR-PDT.

Reticulum Targeting

Another target is the plasma reticulum. The BODIPY **10** (Figure 13) bearing an analogous glibenclamide motif obtained by Zhou et al., has precisely the goal of targeting towards the plasma reticulum [121].

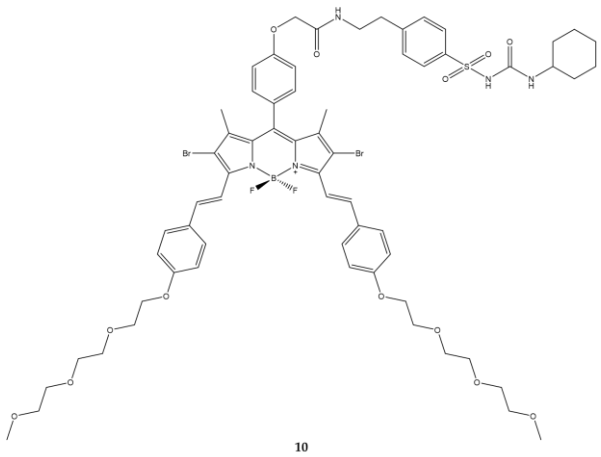

Figure 13. Chemical structures of compound **10** [121].

The absorption spectrum of the compound exhibits the band at 669 nm. The quantity of $^1O_2$ produced by the compound is very low when results were compared to those obtained with the reference molecule, zinc(II) phthalocyanine. The photodynamic activity has been studied on HeLa and HepG2 cells. The light source used is a 300 W halogen lamp on which a colored glass filter has been placed plus a cut-on at λ = 610 nm. The IC_{50} values obtained in both cell lines are lower than 0.2 μM (0.09 μM in HeLa and 0.16 μM in HepG2). Such low concentrations are linked to the high uptake of the compound by the cell lines being analyzed (Table 12).

Table 12. Physico-chemical properties and biological data obtained for compound **10** [121].

	10
λ_{abs} [a]	669 nm
ε	114,815 $M^{-1}cm^{-1}$
λ_{em} [a]	692 nm
Φ_{fluo} [b]	0.32
$^1O_2$ QY [c]	0.11
$IC_{50\ (Hela)}$ [d]	0.09 μM
$IC_{50\ (HepG2)}$ [d]	0.16 μM

[a] In PBS with 0.3% *v*/*v* Tween 80 and 1% *v*/*v* DMF. [b] With reference to zinc(II) phthalocyanine (Φ_{fluo} = 0.28 in DMF). [c] With reference to zinc(II) phthalocyanine ($^1O_2$ QY ≈ 0.56 in DMF). [d] Irradiation with light (λ = 610 nm, 10 min) and dark (50 min) with a total of 24 h of light exposure.

The compound was found to be associated with the endoplasmic reticulum using confocal microscopy when the results were compared to those obtained with cells treated with an analog molecule without glibenclamide. The analog molecule did not accumulate in reticulum.

Mitochondrial Targeting

In 2021 Bhattacheryya et al., thought of binding a iodine-BODIPY to a metallic ternary system to increase its solubility in water, an essential factor for in vivo applications of highly lipophilic molecules [122,123] (Figure 14).

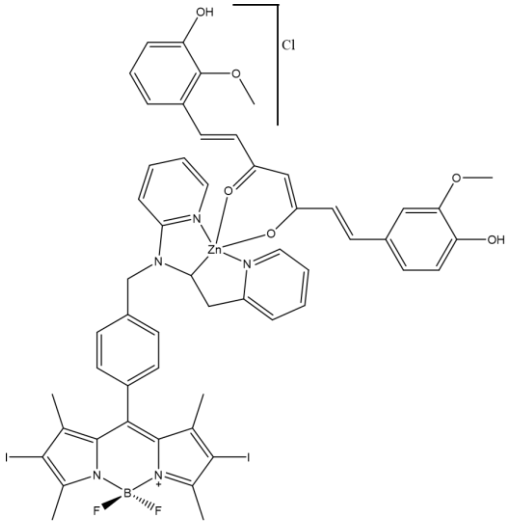

3

Figure 14. Chemical structures of compound **3** [122,123].

Curcumin was further coordinated within the system. Curcumin is well known for its tumor specific activity [124–126] but also as a photosensitizer. Curcumin in the native form has poor bioavailability and is susceptible to hydrolysis under cellular pH conditions thus reducing its therapeutic efficacy. However, curcumin bound to transition metal ions became stable and the metal complexes show significant mitochondrial localization [127]. In this work the authors show that the complex **3** having green light harvesting di-iodinated BODIPY and curcumin for mitochondrial targeting have an interesting photodynamic activity in human breast cancer (MCF7) via disruption of mitochondrial membrane (Table 13).

Table 13. Physico-chemical properties and biological data obtained for compound **3** [122,123].

	3
λ_{abs} [a]	543 nm
ε	29,400 $M^{-1}cm^{-1}$
λ_{em} [a]	506 nm
Φ_{fluo} [b]	0.02
$^1O_2$ QY [c]	0.73
$IC_{50\ (HeLa)}$ [d]	0.025 µM
$IC_{50\ (MCF7)}$ [d]	0.055 µM
$IC_{50\ (HPL1D)}$ [d]	0.230 µM

[a] In 1% DMSO-DPBS buffer medium (pH = 7.4). [b] With fluoresceinf (0.1 M NaOH, Φ_{fluo} = 0.79) as standard. [c] Using Rose Bengal as standard in DMSO ($^1O_2$ QY = 0.76). [d] Irradiation with a visible light source for 1 h (fluence rate = 2.4 mW/cm^2, light dose = 10 J/cm^2).

Cell Membrane Targeting

The targeting can be implemented not only towards cytoplasmic organelles but also towards receptors present on cell plasmic membrane.

The asialoglycoprotein receptor (ASGP) is expressed exclusively in the liver and was considered by Li et al., to design a BODIPY that specifically targeted it [111]. For this purpose, the author has synthesized a new macro-molecular PS equipped with hydrophilic appendix capable of selectively targeting liver cancer cells. The compound obtained is a galactose-functionalized BODIPY-based macromolecular photosensitizer **p(GEMA-co-BODIPYMA)-2I** with good solubility in aqueous environment (Figure 15).

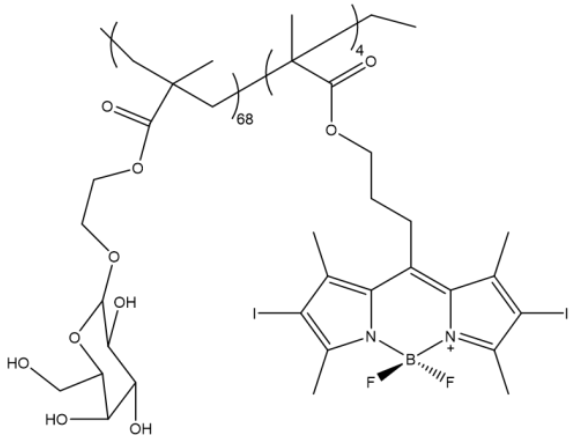

p(GEMA-co-BODIPYMA)-2I

Figure 15. Chemical structures of compound **p(GEMA-co-BODIPYMA)-2I** [111].

The compound proved to be a good $^1O_2$ producer. Biological tests were carried out on HepG2 and NIH3T3 cell lines and first concerned the specific binding towards liver cells and subsequently the cytotoxic activity on them was evaluated (Table 14).

Table 14. Physico-chemical properties and biological data obtained for compound **p(GEMA-co-BODIPYMA)-2I** [111].

	p(GEMA-co-BODIPYMA)-2I
λ_{abs} [a]	535 nm
$^1O_2$ QY [b]	0.79

[a] In H_2O. [b] Rose Bengal ($^1O_2$ = 0.76) was used as reference.

The compound was observed in the cytoplasm of HepG2 cells as demonstrated by confocal microscopy using fluorescence emission of iodine atoms. Previous studies carried out by the same group [128] have shown that the removal of galactose does not allow targeting towards HepG2 cells. The results therefore suggest that the internalization of **p(GEMA-co-BODIPYMA)-2I** depends mainly on the ASGP receptor, over expressed in HepG2 cells. The photodynamic efficacy of the compound was then evaluated. Cell survival was less than 20% following treatment with a concentration lower than 20 μM. In addition, cell exposure to the BODIPY derivative triggered cell to apoptosis. In contrast, the compound did not accumulate in NIH3T3 lacking ASGP receptor expression and the cells did not undergo cell death after light exposure.

Tyrosinase is a key regulatory enzyme in the biosynthesis of melanin through melanogenesis and is localized in the membrane of melanosome. Tyrosinase level is closely correlated with the malignancy level, so it can be considered as a biomarker of melanoma cell. Phenylthiourea (PTU) is one of the most important and well-known tyrosinase inhibitors. Kim et al., designed a BODIPY derivative with PTU pendant to enhance the PDT efficacy against melanoma cell line (Figure 16).

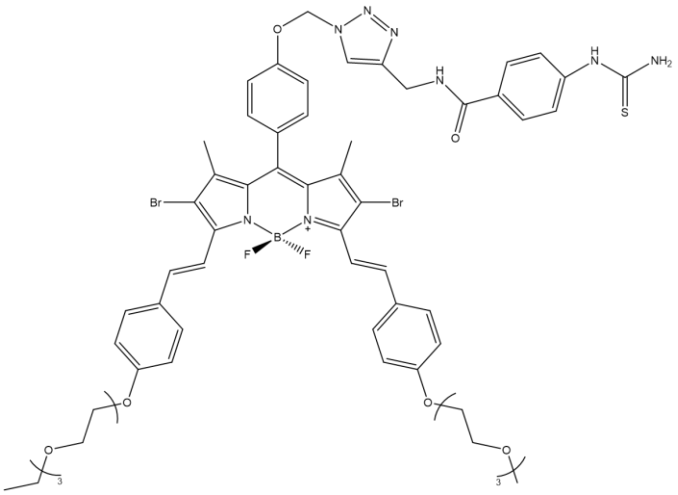

PTUBDP

Figure 16. Chemical structures of compound **PTUBDP** [129].

Cellular uptake studies demonstrated the specificity of the binding of the compound to tyrosinase overexpressed in murine B16F10 cells [129] (Table 15).

Table 15. Physico-chemical properties and biological data obtained for compound **PTUBDP** [129].

	PTUBDP
λ_{abs} [a]	667 nm
ε	54,400 $M^{-1}cm^{-1}$
λ_{em} [a]	712 nm
$^1O_2$ QY [b]	0.093

[a] In DMSO. [b] In DMSO with Rose Bengala as a reference.

Epidermal growth factor (EGFR) is another target since it is expressed in diverse tumor cells. In recent years, a series of sequences able to bind specifically to this receptor have been identified [130]; Zhao et al., selected the sequence namely D4 which was bound to polyethylene glycol and subsequently placed on a BODIPY (Figure 17) [131].

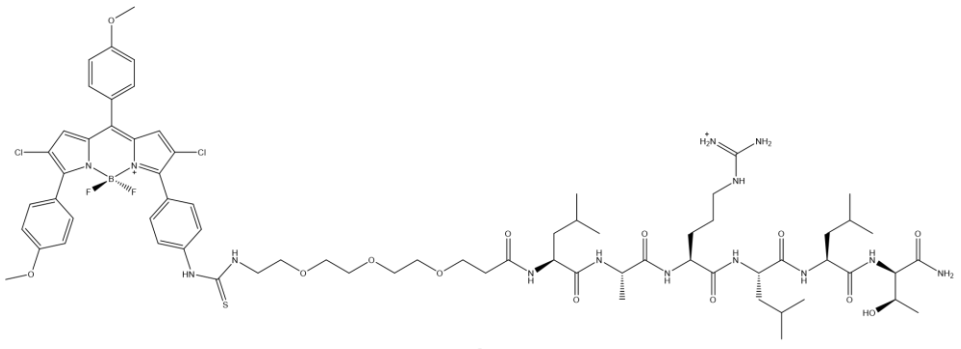

8

Figure 17. Chemical structures of compound **8** [131].

Conjugation with the peptide (**8**) shows a slight shift of the emission and absorption bands with respect to the precursor without the peptide. The quantum yield of fluorescence is five times lower than that of the compound without the peptide (Table 16).

Table 16. Physico-chemical properties and biological data obtained for compound **8** [131].

	8
λ_{abs} [a]	588 nm
ε	43,000 $M^{-1}cm^{-1}$
λ_{em} [a]	634 nm
Φ_{fluo} [b]	0.003
$IC_{50\ (HepG2)}$ [c]	74 µM

[a] In DMSO. [b] Cresyl Violet (Φfluo ≈ 0.50 in ethanol) as a reference. [c] Irradiation with halogen lamp for 20 min with a light dose of 1.5 J/cm^2.

Photodynamic activity data on HepG2 human carcinoma cell, known to express EGFR [132,133] studies show that the conjugate is more active than the precursor without the peptide this is probably due to the presence of a positive charge on the peptide sequence which should favor a faster and more efficient cell internalization [134]. Uptake kinetic demonstrated a fast absorption of the molecule over 24 h, suggesting that the presence of triethylene glycol and the positive charge of the peptide sequence increase the internalization of the compound.

Burgess et al. worked on targeting the receptor tyrosine kinase [135–137]. Starting from a series of previous experiments in which specific conjugates for the receptor tyrosine kinase with cytotoxicity were identified, Burgess decided to hook these conjugates to a BODIPY to obtain a molecule (**IY-IY-PDT**) (Figure 18) usable in PDT [136].

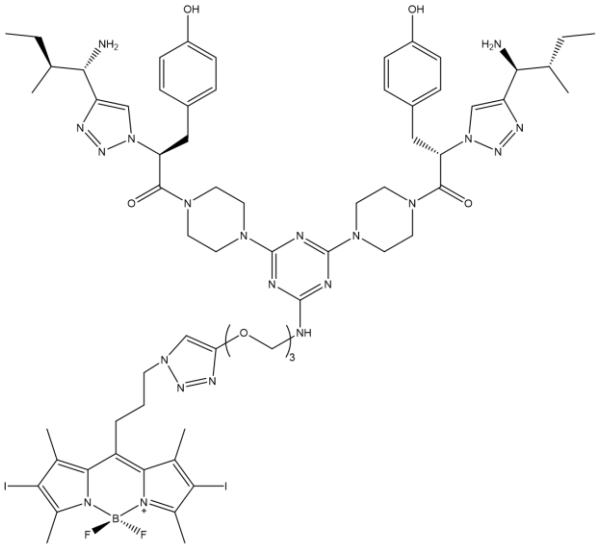

Figure 18. Chemical structures of compound **1** (**IY-IY-PDT**) [135].

Following the satisfactory results of the physico-chemical characterization, the molecule obtained was tested on NIHT3T wild-type (NIHT3T-WT) and over cell lines expressing the receptor tyrosine kinase (NIHT3T-TrkC). It was possible to detect a significant photo-induced cytotoxicity effect in over-expressing cells following treatment with the compound **IY-IY-PDT** (IC_{50} = 0.35 µM) (Table 17).

Table 17. Physico-chemical properties and biological data obtained for compound **1** (**IY-IY-PDT**) [135].

	IY-IY-PDT
λ_{abs} [a]	532 nm
λ_{em} [a]	550 nm
$IC_{50\ (NIH3T3)}$ [b]	0.35 μM

[a] In DMSO. [b] Irradiation with a halogen lamp for 10 min with a light dose of 7.3 J/cm$^{2.}$

In cellular localization it states that the compound under analysis is mainly located at the level of the lysosomes while it does not accumulate at the mitochondrial or endoplasmic reticulum level by exploiting the tyrosine kinase receptor.

The following year, the same author tested the same compound on breast cancer cell lines expressing receptor tyrosine kinase [136]. The data obtained also in this case affirm that the compound is more assimilated by the cells that express the receptor and also in this case the localization of the compound is at the lysosomal level. The first in vivo tests on mice are also carried out in this article which showed that there is a high decrease in tumor size in mice starting at four days of illumination.

In the next article published in 2016, the author reports an increased antitumor immune response after treatment with the conjugate and illumination of the area of interest [137]. The overall analysis of the data reported in the three articles published by the author leads to the hypothesis that the compound **IY-IY-PDT** acts as a therapeutic agent capable of stimulating the immune system, which makes it an excellent candidate for use in clinical practice of cancer treatment.

2.4. Sensitive Activity

Another area in which the research was concentrated was that of obtaining BODIPYs capable of being activated in specific conditions such as acid pH, typical of cancer cells, or in the presence of particular molecules such as glutathione (GSH).

Radunz et al. evaluated the activity of a pH-activable fluorescent $^1O_2$ generating BODIPY dyes (**3b**), which can be used as PS and for bioimaging (Figure 19) [138].

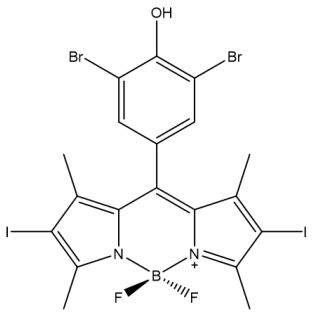

3b

Figure 19. Chemical structures of compound **3b** [138].

To ensure that the compound was able to produce a high level of $^1O_2$, the core of the BODIPY has iodine atoms in *β*-positions. The responsive part of the pH is instead represented by a phenolic substituent placed in the meso position of the core.

From the titrations carried out in the pH range between 4.5 and 8.2 it is observed that the absorption is minimally influenced by the pH while the intensity of the fluorescence decreases drastically at basic pH. The production of $^1O_2$ is shown in Table 18.

Table 18. Physico-chemical properties and biological data obtained for compound **3b** [138].

	3b
λ_{abs} [a]	534 nm
ε	99,000 $M^{-1}cm^{-1}$
λ_{em} [a]	550 nm
Φ_{fluo}	0.02
$^1O_2$ QY [b]	0.59
$IC_{50\ (HeLa)}$ [c]	70 nM
$IC_{50\ (HeLa,\ pH=5.5)}$ [d]	30 nM
$IC_{50\ (HeLa,\ pH=7.5)}$ [d]	150 nM

[a] In acetonitrile. [b] With DPBF as indicator and Rose Bengala as standard. [c] Irradiation with laser diode (λ = 532 nm) for 30 min. [d] Irradiation with laser diode (λ = 532 nm) for 5 min with an irradiance of 1 mW/cm^2.

As a result of the irradiation the compound showed an activity with an IC_{50} on the HeLa tumor cell line equal to 70 nM. The authors repeated the photodynamic experiment by adjusting the intracellular pH to a value of 5.5 or 7.5 before illumination [138]. The results obtained showed that cell survival was lower for cells with an acidic environment compared to those in a neutral environment (cell survival was 10% vs. 70% at a PS concentration of 0.1 μM).

Cao et al. reported the synthesis of a GSH-responsive BODIPY (**8a**) consisting of three modules: a BODIPY-based photosensitizing chromophore, a BODIPY-based quencher and a bio-reducible disulfide linker (Figure 20) [139].

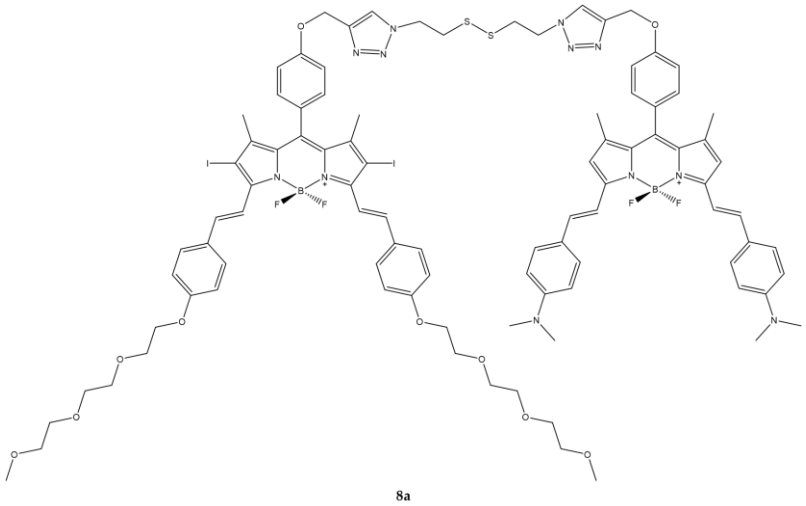

8a

Figure 20. Chemical structures of compound **8a** [139].

The compound thus obtained has shown to have excellent photophysical and photochemical characteristics such as a strong absorption in the visible region and in the NIR as well as high photostability. Overall, the compound does not show fluorescence, but after the addition of 10 μM of GSH which breaks the disulfide bond, the fluorescence is recovered.

In vitro studies have been conducted on three cell lines (A549, H22 and HeLa) known to have high intracellular concentrations of GSH. The compound is rapidly internalized by cells and effectively activated by intracellular biothiols. In the presence of light, the activity expressed as IC_{50} is of the order of μM. The compound is mainly localized in mitochondria where it is believed that GSH-mediated cleavage may also occur (Table 19).

Table 19. Physico-chemical properties and biological data obtained for compound **8a** [139].

	8a
λ_{abs} [a]	664 nm
λ_{em} [a]	768 nm
Φ_{fluo} [b]	0.052
$^1O_2$ QY [c]	0.018
$IC_{50\ (HeLa)}$ [d]	0.67 μM
$IC_{50\ (A549)}$ [d]	0.44 μM
$IC_{50\ (H22)}$ [d]	0.48 μM

[a] In DMF. [b] Relative to unsubstituted zinc(II) phthalocyanine in DMF as the reference (Φfluo ≈ 0.28). [c] Relative to unsubstituted zinc(II) phthalocyanine ($^1O_2$ QY ≈ 0.56). [d] Irradiation with a 670 nm LED lamp for 2 min with an irradiance of 20 mW/cm^2.

In vivo experiments on H22 tumor-bearing mice showed high selectivity in tumor tissue and efficacy in inhibiting tumor growth.

Jiang et al., synthetized a BODIPY responsive to both pH and thiol groups [140]. Specifically, compound (**7**) has two ferrocenyl moieties attached to a combination of ketal- and disulfide-linkers (Figure 21). The former is cleaved in acid conditions, while the latter with cellular GSH.

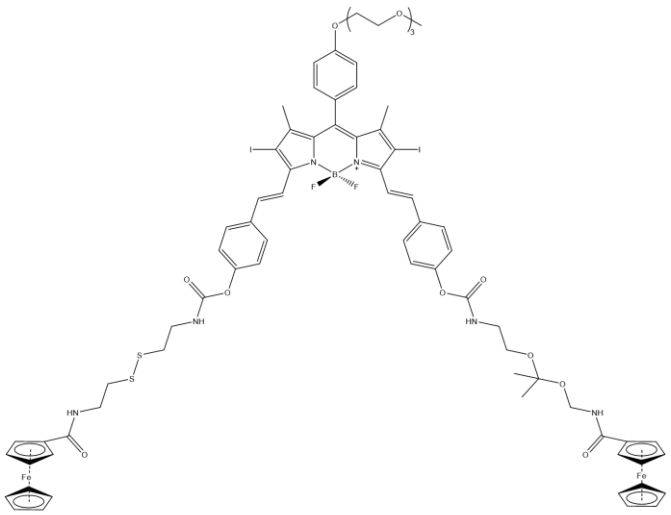

7

Figure 21. Chemical structures of compound **7** [140].

Fluorescence and $^1O_2$ production of the molecule depends on the two ferrocenyl groups, in fact at acid pH and in the presence of GSH, which break the ketal and the disulfide bond, an increase in fluorescence and $^1O_2$ is observed (Table 20).

Table 20. Physico-chemical properties and biological data obtained for compound **7** [140].

	7
λ_{abs} [a]	376, 441, 662 nm
λ_{em} [a]	686 nm
Φ_{fluo} [a]	0.03
$IC_{50\ (MCF7,\ no\ DTT}$ [b]	146.0 nM
$IC_{50\ ((MCF7,\ 2\ \mu M\ DTT)}$ [b]	140.0 nM
$IC_{50\ (MCF7,\ 4\ mM\ DTT)}$ [b]	81 nM

[a] In PBS with 0.25% Cremophor EL. [b] Irradiation with a halogen lamp for 20 min with a total fluence of 48 J/cm^2.

Photodynamic activity studies on the MCF7 cell line showed that compound **7** has dithiothreitol (DTT) dependent behavior (IC_{50} halves when DTT goes from 2 μM to 4 mM).

In vivo experiments were conducted using nude mice carrying HT29 human colorectal carcinoma. From the fluorescence images it is observed that compound **7** is localized only and exclusively in the area of the tumor, suggesting that the compound is activated only and exclusively at the tumor level where there is the cleavage of the two linkers, by means of pH and DTT, and consequent detachment of the two ferrocenyl motifs.

Funding: This research received no external funding.

Conflicts of Interest: The authors declare no conflict of interest.

References

1. Dougherty, T.J.; Gomer, C.J.; Henderson, B.W.; Jori, G.; Kessel, D.; Korbelik, M.; Moan, J.; Peng, Q. Photodynamic therapy. *J. Natl. Cancer Inst.* **1998**, *90*, 889–905. [CrossRef] [PubMed]
2. Chilakamarthi, U.; Giribabu, L. Photodynamic Therapy: Past, Present and Future. *Chem. Rec.* **2017**, *17*, 775–802. [CrossRef] [PubMed]
3. Blum, H.F. Photodynamic action and diseases caused by light. *Am. Chem. Soc. Monogr.* **1941**, *85*, 283–295. [CrossRef]
4. Zhou, Z.; Song, J.; Nie, L.; Chen, X. Reactive oxygen species generating systems meeting challenges of photodynamic cancer therapy. *Chem. Soc. Rev.* **2016**, *45*, 6597–6626. [CrossRef] [PubMed]
5. Allison, R.R.; Downie, G.H.; Cuenca, R.; Hu, X.H.; Childs, C.J.; Sibata, C.H. Photosensitizers in clinical PDT. *Photodiagnosis Photodyn. Ther.* **2004**, *1*, 27–42. [CrossRef]
6. Juzeniene, A.; Peng, Q.; Moan, J. Milestones in the development of photodynamic therapy and fluorescence diagnosis. *Photochem. Photobiol. Sci.* **2007**, *6*, 1234–1245. [CrossRef]
7. Daniell, M.D.; Hill, J.S. A history of photodynamic therapy. *Aust. N. Z. J. Surg.* **1991**, *61*, 340–348. [CrossRef] [PubMed]
8. Castellani, A.; Pace, G.P.; Concioli, M. Photodynamic effect of haematoporphyrin on blood microcirculation. *J. Pathol. Bacteriol.* **1963**, *86*, 99–102. [CrossRef] [PubMed]
9. de Gruijl, F.R.; Van der Leun, J.C. Estimate of the wavelength dependency of ultraviolet carcinogenesis in humans and its relevance to the risk assessment of a stratospheric ozone depletion. *Health Phys.* **1994**, *67*, 319–325. [CrossRef]
10. Dolmans, D.E.; Fukumura, D.; Jain, R.K. Photodynamic therapy for cancer. *Nat. Rev. Cancer* **2003**, *3*, 380–387. [CrossRef]
11. Agostinis, P.; Berg, K.; Cengel, K.A.; Foster, T.H.; Girotti, A.W.; Gollnick, S.O.; Hahn, S.M.; Hamblin, M.R.; Juzeniene, A.; Kessel, D.; et al. Photodynamic therapy of cancer: An update. *CA Cancer J. Clin.* **2011**, *61*, 250–281. [CrossRef] [PubMed]
12. Ledoux-Lebards, C. Action de la lumiere sur la toxicite de l'éosine et de quelques autres substances. *Ann. Inst. Pasteur* **1902**, *16*, 587–593.
13. Foote, C.S. Mechanisms of photosensitized oxidation. There are several different types of photosensitized oxidation which may be important in biological systems. *Science* **1968**, *162*, 963–970. [CrossRef] [PubMed]
14. Moan, J.; Wold, E. Detection of singlet oxygen production by ESR. *Nature* **1979**, *279*, 450–451. [CrossRef] [PubMed]
15. Moan, J.; Sommer, S. Oxygen dependence of the photosensitizing effect of hematoporphyrin derivative in NHIK 3025 cells. *Cancer Res.* **1985**, *45*, 1608–1610. [PubMed]
16. Devasagayam, T.P.A.; Kamat, J.P. Biological significance of singlet oxygen. *Indian J. Exp. Biol.* **2002**, *40*, 680–692.
17. Davies, M.J. Singlet oxygen-mediated damage to proteins and its consequences. *Biochem. Biophys. Res. Commun.* **2003**, *305*, 761–770. [CrossRef]
18. Juzeniene, A.; Nielsen, K.P.; Moan, J. Biophysical aspects of photodynamic therapy. *J. Environ. Pathol. Toxicol. Oncol.* **2006**, *25*, 7–28. [CrossRef] [PubMed]
19. Schmidt, R. Photosensitized Generation of Singlet Oxygen. *Photochem. Photobiol.* **2007**, *82*, 1161–1177. [CrossRef]
20. Sharman, W.M.; Allen, C.M.; van Lier, J.E. Role of activated oxygen species in photodynamic therapy. *Methods Enzymol.* **2000**, *319*, 376–400. [CrossRef]
21. Li, C. *Breast Cancer Epidemiology*, 1st ed.; Springer: New York, NY, USA, 2010; pp. 1–417.
22. Castano, A.P.; Demidova, T.N.; Hamblin, M.R. Mechanisms in photodynamic therapy: Part one-photosensitizers, photochemistry and cellular localization. *Photodiagnosis Photodyn. Ther.* **2004**, *1*, 279–293. [CrossRef]
23. Robertson, C.A.; Evans, D.H.; Abrahamse, H. Photodynamic therapy (PDT): A short review on cellular mechanisms and cancer research applications for PDT. *J. Photochem. Photobiol. B* **2009**, *96*, 1–8. [CrossRef] [PubMed]
24. Kwiatkowski, S.; Knap, B.; Przystupski, D.; Saczko, J.; Kedzierska, E.; Knap-Czop, K.; Kotlinska, J.; Michel, O.; Kotowski, K.; Kulbacka, J. Photodynamic therapy-mechanisms, photosensitizers and combinations. *Biomed. Pharmacother.* **2018**, *106*, 1098–1107. [CrossRef] [PubMed]
25. Schenck, G.O. Photosensitized reactions with molecular oxygen. *Naturwissenschaften* **1984**, *71*, 28–29.
26. Foote, C.S.; Wexler, S. Singlet Oxygen. A Probable Intermediate in Photosensitized Autoxidations. *J. Am. Chem. Soc.* **2002**, *86*, 3880–3881. [CrossRef]
27. Niedre, M.J.; Secord, A.J.; Patterson, M.S.; Wilson, B.C. In vitro tests of the validity of singlet oxygen luminescence measurements as a dose metric in photodynamic therapy. *Cancer Res.* **2003**, *63*, 7986–7994. [PubMed]

28. Weishaupt, K.R.; Gomer, C.J.; Dougherty, T.J. Identification of singlet oxygen as the cytotoxic agent in photoinactivation of a murine tumor. *Cancer Res.* **1976**, *36*, 2326–2329.
29. Fisher, A.M.; Murphree, A.L.; Gomer, C.J. Clinical and preclinical photodynamic therapy. *Lasers Surg. Med.* **1995**, *17*, 2–31. [CrossRef]
30. Dos Santos, A.F.; Terra, L.F.; Wailemann, R.A.M.; Oliveira, T.C.; de Morais Gomes, V.; Mineiro, M.F.; Meotti, F.C.; Bruni-Cardoso, A.; Baptista, M.S.; Labriola, L. Methylene blue photodynamic therapy induces selective and massive cell death in human breast cancer cells. *BMC Cancer* **2017**, *17*, 194–209. [CrossRef]
31. Auten, R.L.; Davis, J.M. Oxygen toxicity and reactive oxygen species: The devil is in the details. *Pediatr. Res.* **2009**, *66*, 121–127. [CrossRef]
32. van Duijnhoven, F.H.; Aalbers, R.I.; Rovers, J.P.; Terpstra, O.T.; Kuppen, P.J. The immunological consequences of photodynamic treatment of cancer, a literature review. *Immunobiology* **2003**, *207*, 105–113. [CrossRef]
33. Mroz, P.; Hashmi, J.T.; Huang, Y.Y.; Lange, N.; Hamblin, M.R. Stimulation of anti-tumor immunity by photodynamic therapy. *Expert Rev. Clin. Immunol.* **2011**, *7*, 75–91. [CrossRef] [PubMed]
34. Mroz, P.; Hamblin, M.R. The immunosuppressive side of PDT. *Photochem. Photobiol. Sci.* **2011**, *10*, 751–758. [CrossRef] [PubMed]
35. Reginato, E.; Wolf, P.; Hamblin, M.R. Immune response after photodynamic therapy increases anti-cancer and anti-bacterial effects. *World J. Immunol.* **2014**, *4*, 1–11. [CrossRef] [PubMed]
36. Lobo, A.C.S.; Gomes-da-Silva, L.C.; Rodrigues-Santos, P.; Cabrita, A.; Santos-Rosa, M.; Arnaut, L.G. Immune Responses after Vascular Photodynamic Therapy with Redaporfin. *J. Clin. Med.* **2019**, *9*, 104. [CrossRef] [PubMed]
37. Falk-Mahapatra, R.; Gollnick, S.O. Photodynamic Therapy and Immunity: An Update. *Photochem. Photobiol.* **2020**, *96*, 550–559. [CrossRef]
38. Nkune, N.W.; Simelane, N.W.N.; Montaseri, H.; Abrahamse, H. Photodynamic Therapy-Mediated Immune Responses in Three-Dimensional Tumor Models. *Int. J. Mol. Sci.* **2021**, *22*, 12618. [CrossRef]
39. Gilchrest, B.A. Photodynamic therapy and selected off-label uses. In *Winter Clinical Dermatology Conference-Hawaii*; Tuleya, S., Ed.; HMP Communications, LLC: Kohala Coast, HI, USA, 2010; pp. 10–12.
40. Kamkaew, A.; Lim, S.H.; Lee, H.B.; Kiew, L.V.; Chung, L.Y.; Burgess, K. BODIPY dyes in photodynamic therapy. *Chem. Soc. Rev.* **2013**, *42*, 77–88. [CrossRef]
41. Liu, J.; Zheng, L.; Li, Y.; Zhang, Z.; Zhang, L.; Shen, L.; Zhang, X.; Qiao, H. Effect of DTPP-mediated photodynamic therapy on cell morphology, viability, cell cycle, and cytotoxicity in a murine lung adenocarcinoma cell line. *Lasers Med. Sci.* **2015**, *30*, 181–191. [CrossRef]
42. Meyer-Betz, F. Untersuchungen uber die biologische (photodynamische) Wirkung des Hamatoporphyrings und anderer Derivate des Blut- und Gallenfarbstoffs. *Dtsch. Arch. Klin. Med.* **1913**, *112*, 476–503.
43. Ackroyd, R.; Kelty, C.; Brown, N.; Reed, M. The history of photodetection and photodynamic therapy. *Photochem. Photobiol.* **2001**, *74*, 656–669. [CrossRef]
44. Ormond, A.B.; Freeman, H.S. Dye Sensitizers for Photodynamic Therapy. *Materials* **2013**, *6*, 817–840. [CrossRef] [PubMed]
45. Hage, R.; Ferreira, J.; Bagnato, V.S.; Vollet, E.D.; Plapler, H. Pharmacokinetics of Photogem Using Fluorescence Spectroscopy in Dimethylhydrazine-Induced Murine Colorectal Carcinoma. *Int. J. Photoenergy* **2012**, *2012*, 1–8. [CrossRef]
46. Allison, R.R.; Sibata, C.H. Oncologic photodynamic therapy photosensitizers: A clinical review. *Photodiagnosis Photodyn. Ther.* **2010**, *7*, 61–75. [CrossRef] [PubMed]
47. Hammerer, F.; Poyer, F.; Fourmois, L.; Chen, S.; Garcia, G.; Teulade-Fichou, M.P.; Maillard, P.; Mahuteau-Betzer, F. Mitochondria-targeted cationic porphyrin-triphenylamine hybrids for enhanced two-photon photodynamic therapy. *Bioorganic Med. Chem.* **2018**, *26*, 107–118. [CrossRef] [PubMed]
48. Gilson, D.; Ash, D.; Driver, I.; Feather, J.W.; Brown, S. Therapeutic ratio of photodynamic therapy in the treatment of superficial tumours of skin and subcutaneous tissues in man. *Br. J. Cancer* **1988**, *58*, 665–667. [CrossRef] [PubMed]
49. Hausser, K.W.; Vahle, W. Die abhangigkeit des lichterythems und der pigmentbildung von der schwingungszahl (wellenlange der erregenden strahlung). *Strahlentherapie* **1931**, *13*, 41–71.
50. Chevalier, S.; Anidjar, M.; Scarlata, E.; Hamel, L.; Scherz, A.; Ficheux, H.; Borenstein, N.; Fiette, L.; Elhilali, M. Preclinical study of the novel vascular occluding agent, WST11, for photodynamic therapy of the canine prostate. *J. Urol.* **2011**, *186*, 302–309. [CrossRef]
51. Triesscheijn, M.; Ruevekamp, M.; Aalders, M.; Baas, P.; Stewart, F.A. Outcome of mTHPC mediated photodynamic therapy is primarily determined by the vascular response. *Photochem. Photobiol.* **2005**, *81*, 1161–1167. [CrossRef]
52. Detty, M.R.; Gibson, S.L.; Wagner, S.J. Current clinical and preclinical photosensitizers for use in photodynamic therapy. *J. Med. Chem.* **2004**, *47*, 3897–3915. [CrossRef]
53. Dovigo, L.N.; Pavarina, A.C.; Ribeiro, A.P.; Brunetti, I.L.; Costa, C.A.; Jacomassi, D.P.; Bagnato, V.S.; Kurachi, C. Investigation of the photodynamic effects of curcumin against Candida albicans. *Photochem. Photobiol.* **2011**, *87*, 895–903. [CrossRef]
54. Wohrle, D.; Hirth, A.; Bogdahn-Rai, T.; Schnurpfeil, G.; Shopova, M. Photodynamic therapy of cancer: Second and third generations of photosensitizers. *Russ. Chem. Bull.* **1998**, *47*, 807–816. [CrossRef]
55. Li, L.; Nguyen, B.; Burgess, K. Functionalization of the 4,4-difluoro-4-bora-3a,4a-diaza-s-indacene (BODIPY) core. *Bioorganic Med. Chem. Lett.* **2008**, *18*, 3112–3116. [CrossRef] [PubMed]

56. Awuah, S.G.; You, Y. Boron dipyrromethene (BODIPY)-based photosensitizers for photodynamic therapy. *RSC Adv.* **2012**, *2*, 11169–11183. [CrossRef]
57. Yuster, P.; Weissman, S.I. Effects of Perturbations on Phosphorescence: Luminescence of Metal Organic Complexes. *J. Chem. Phys.* **1949**, *17*, 1182–1188. [CrossRef]
58. Treibs, A.; Kreuzer, F.-H. Difluorboryl-Komplexe von Di- und Tripyrrylmethenen. *Justus Liebigs Ann. Chem.* **1968**, *718*, 208–223. [CrossRef]
59. Ulrich, G.; Ziessel, R.; Harriman, A. The chemistry of fluorescent bodipy dyes: Versatility unsurpassed. *Angew. Chem. Int. Ed. Engl.* **2008**, *47*, 1184–1201. [CrossRef]
60. Karolin, J.; Johansson, L.B.A.; Strandberg, L.; Ny, T. Fluorescence and Absorption Spectroscopic Properties of Dipyrrometheneboron Difluoride (BODIPY) Derivatives in Liquids, Lipid Membranes, and Proteins. *J. Am. Chem. Soc.* **2002**, *116*, 7801–7806. [CrossRef]
61. Yogo, T.; Urano, Y.; Ishitsuka, Y.; Maniwa, F.; Nagano, T. Highly efficient and photostable photosensitizer based on BODIPY chromophore. *J. Am. Chem. Soc.* **2005**, *127*, 12162–12163. [CrossRef]
62. Wittmershaus, B.P.; Skibicki, J.J.; McLafferty, J.B.; Zhang, Y.-Z.; Swan, S. Spectral properties of single BODIPY dyes in polystyrene microspheres and in solutions. *J. Fluoresc.* **2001**, *11*, 119–128. [CrossRef]
63. Ventura, B.; Marconi, G.; Bröring, M.; Krüger, R.; Flamigni, L. Bis(BF2)-2,2′-bidipyrrins, a class of BODIPY dyes with new spectroscopic and photophysical properties. *New J. Chem.* **2009**, *33*, 428–438. [CrossRef]
64. Kolemen, S.; Bozdemir, O.A.; Cakmak, Y.; Barin, G.; Erten-Ela, S.; Marszalek, M.; Yum, J.-H.; Zakeeruddin, S.M.; Nazeeruddin, M.K.; Grätzel, M.; et al. Optimization of distyryl-Bodipy chromophores for efficient panchromatic sensitization in dye sensitized solar cells. *Chem. Sci.* **2011**, *2*, 949–954. [CrossRef]
65. Koziar, J.C.; Cowan, D.O. Photochemical heavy-atom effects. *Acc. Chem. Res.* **2002**, *11*, 334–341. [CrossRef]
66. Loudet, A.; Burgess, K. BODIPY dyes and their derivatives: Syntheses and spectroscopic properties. *Chem. Rev.* **2007**, *107*, 4891–4932. [CrossRef] [PubMed]
67. Banfi, S.; Nasini, G.; Zaza, S.; Caruso, E. Synthesis and photo-physical properties of a series of BODIPY dyes. *Tetrahedron* **2013**, *69*, 4845–4856. [CrossRef]
68. Shivran, N.; Tyagi, M.; Mula, S.; Gupta, P.; Saha, B.; Patro, B.S.; Chattopadhyay, S. Syntheses and photodynamic activity of some glucose-conjugated BODIPY dyes. *Eur. J. Med. Chem.* **2016**, *122*, 352–365. [CrossRef] [PubMed]
69. DeRosa, M. Photosensitized singlet oxygen and its applications. *Coord. Chem. Rev.* **2002**, *233–234*, 351–371. [CrossRef]
70. Fagnoni, M. Modern Molecular Photochemistry of Organic Molecules. By Nicholas J. Turro, V. Ramamurthy and Juan C. Scaiano. *Angew. Chem. Int. Ed.* **2010**, *49*, 6709–6710. [CrossRef]
71. Pham, T.C.; Nguyen, V.N.; Choi, Y.; Lee, S.; Yoon, J. Recent Strategies to Develop Innovative Photosensitizers for Enhanced Photodynamic Therapy. *Chem. Rev.* **2021**, *121*, 13454–13619. [CrossRef]
72. Banfi, S.; Caruso, E.; Zaza, S.; Mancini, M.; Gariboldi, M.B.; Monti, E. Synthesis and photodynamic activity of a panel of BODIPY dyes. *J. Photochem. Photobiol. B* **2012**, *114*, 52–60. [CrossRef]
73. Banfi, S.; Caruso, E.; Buccafurni, L.; Murano, R.; Monti, E.; Gariboldi, M.; Papa, E.; Gramatica, P. Comparison between 5,10,15,20-tetraaryl- and 5,15-diarylporphyrins as photosensitizers: Synthesis, photodynamic activity, and quantitative structure-activity relationship modeling. *J. Med. Chem.* **2006**, *49*, 3293–3304. [CrossRef]
74. Frimayanti, N.; Yam, M.L.; Lee, H.B.; Othman, R.; Zain, S.M.; Rahman, N.A. Validation of quantitative structure-activity relationship (QSAR) model for photosensitizer activity prediction. *Int. J. Mol. Sci.* **2011**, *12*, 8626–8644. [CrossRef] [PubMed]
75. Henderson, B.W.; Bellnier, D.A.; Greco, W.R.; Sharma, A.; Pandey, R.K.; Vaughan, L.A.; Weishaupt, K.R.; Dougherty, T.J. An in vivo quantitative structure-activity relationship for a congeneric series of pyropheophorbide derivatives as photosensitizers for photodynamic therapy. *Cancer Res.* **1997**, *57*, 4000–4007.
76. Margaron, P.; Gregoire, M.J.; Scasnar, V.; Ali, H.; van Lier, J.E. Structure-photodynamic activity relationships of a series of 4-substituted zinc phthalocyanines. *Photochem. Photobiol.* **1996**, *63*, 217–223. [CrossRef] [PubMed]
77. Zagami, R.; Sortino, G.; Caruso, E.; Malacarne, M.C.; Banfi, S.; Patane, S.; Monsu Scolaro, L.; Mazzaglia, A. Tailored-BODIPY/Amphiphilic Cyclodextrin Nanoassemblies with PDT Effectiveness. *Langmuir* **2018**, *34*, 8639–8651. [CrossRef] [PubMed]
78. Barut, B.; Yalcin, C.O.; Sari, S.; Coban, O.; Keles, T.; Biyiklioglu, Z.; Abudayyak, M.; Demirbas, U.; Ozel, A. Novel water soluble BODIPY compounds: Synthesis, photochemical, DNA interaction, topoisomerases inhibition and photodynamic activity properties. *Eur. J. Med. Chem.* **2019**, *183*, 111685. [CrossRef] [PubMed]
79. Wang, C.; Qian, Y. A water soluble carbazolyl-BODIPY photosensitizer with an orthogonal D-A structure for photodynamic therapy in living cells and zebrafish. *Biomater. Sci.* **2020**, *8*, 830–836. [CrossRef]
80. Caruso, E.; Orlandi, V.T.; Malacarne, M.C.; Martegani, E.; Scanferla, C.; Pappalardo, D.; Vigliotta, G.; Izzo, L. Bodipy-Loaded Micelles Based on Polylactide as Surface Coating for Photodynamic Control of Staphylococcus aureus. *Coatings* **2021**, *11*, 223. [CrossRef]
81. Turan, I.S.; Cakmak, F.P.; Yildirim, D.C.; Cetin-Atalay, R.; Akkaya, E.U. Near-IR absorbing BODIPY derivatives as glutathione-activated photosensitizers for selective photodynamic action. *Chemistry* **2014**, *20*, 16088–16092. [CrossRef]
82. Malacarne, M.C.; Banfi, S.; Caruso, E. In vitro photodynamic treatment of cancer cells induced by aza-BODIPYs. *Photochem. Photobiol. Sci.* **2020**, *19*, 790–799. [CrossRef]

83. Lincoln, R.; Van Kessel, A.T.M.; Zhang, W.; Cosa, G. A dormant BODIPY-acrolein singlet oxygen photosensitizer intracellularly activated upon adduct formation with cysteine residues. *Photochem. Photobiol. Sci.* **2019**, *18*, 2003–2011. [CrossRef]
84. Prieto-Montero, R.; Prieto-Castaneda, A.; Sola-Llano, R.; Agarrabeitia, A.R.; Garcia-Fresnadillo, D.; Lopez-Arbeloa, I.; Villanueva, A.; Ortiz, M.J.; de la Moya, S.; Martinez-Martinez, V. Exploring BODIPY Derivatives as Singlet Oxygen Photosensitizers for PDT. *Photochem. Photobiol.* **2020**, *96*, 458–477. [CrossRef] [PubMed]
85. Ziessel, R.; Ulrich, G.; Harriman, A. The chemistry of Bodipy: A new El Dorado for fluorescence tools. *New J. Chem.* **2007**, *31*, 496–501. [CrossRef]
86. Caruso, E.; Gariboldi, M.; Sangion, A.; Gramatica, P.; Banfi, S. Synthesis, photodynamic activity, and quantitative structure-activity relationship modelling of a series of BODIPYs. *J. Photochem. Photobiol. B* **2017**, *167*, 269–281. [CrossRef] [PubMed]
87. Caruso, E.; Malacarne, M.C.; Marras, E.; Papa, E.; Bertato, L.; Banfi, S.; Gariboldi, M.B. New BODIPYs for photodynamic therapy (PDT): Synthesis and activity on human cancer cell lines. *Bioorganic Med. Chem.* **2020**, *28*, 115737. [CrossRef] [PubMed]
88. Ballestri, M.; Caruso, E.; Guerrini, A.; Ferroni, C.; Banfi, S.; Gariboldi, M.; Monti, E.; Sotgiu, G.; Varchi, G. Core-shell poly-methyl methacrylate nanoparticles covalently functionalized with a non-symmetric porphyrin for anticancer photodynamic therapy. *J. Photochem. Photobiol. B* **2018**, *186*, 169–177. [CrossRef] [PubMed]
89. Kim, B.; Sui, B.; Yue, X.; Tang, S.; Tichy, M.G.; Belfield, K.D. In Vitro Photodynamic Studies of a BODIPY-Based Photosensitizer. *Eur. J. Org. Chem.* **2016**, *2017*, 25–28. [CrossRef]
90. Lincoln, R.; Durantini, A.M.; Greene, L.E.; Martinez, S.R.; Knox, R.; Becerra, M.C.; Cosa, G. meso-Acetoxymethyl BODIPY dyes for photodynamic therapy: Improved photostability of singlet oxygen photosensitizers. *Photochem. Photobiol. Sci.* **2017**, *16*, 178–184. [CrossRef]
91. Durantini, A.M.; Greene, L.E.; Lincoln, R.; Martinez, S.R.; Cosa, G. Reactive Oxygen Species Mediated Activation of a Dormant Singlet Oxygen Photosensitizer: From Autocatalytic Singlet Oxygen Amplification to Chemicontrolled Photodynamic Therapy. *J. Am. Chem. Soc.* **2016**, *138*, 1215–1225. [CrossRef]
92. Epelde-Elezcano, N.; Martínez-Martínez, V.; Peña-Cabrera, E.; Gómez-Durán, C.F.A.; Arbeloa, I.L.; Lacombe, S. Modulation of singlet oxygen generation in halogenated BODIPY dyes by substitution at their meso position: Towards a solvent-independent standard in the vis region. *RSC Adv.* **2016**, *6*, 41991–41998. [CrossRef]
93. Turan, I.S.; Yildiz, D.; Turksoy, A.; Gunaydin, G.; Akkaya, E.U. A Bifunctional Photosensitizer for Enhanced Fractional Photodynamic Therapy: Singlet Oxygen Generation in the Presence and Absence of Light. *Angew. Chem. Int. Ed. Engl.* **2016**, *55*, 2875–2878. [CrossRef]
94. Poully, J.C.; Schermann, J.P.; Nieuwjaer, N.; Lecomte, F.; Gregoire, G.; Desfrancois, C.; Garcia, G.A.; Nahon, L.; Nandi, D.; Poisson, L.; et al. Photoionization of 2-pyridone and 2-hydroxypyridine. *Phys. Chem. Chem. Phys.* **2010**, *12*, 3566–3572. [CrossRef] [PubMed]
95. Matsumoto, M.; Yamada, M.; Watanabe, N. Reversible 1,4-cycloaddition of singlet oxygen to N-substituted 2-pyridones: 1,4-endoperoxide as a versatile chemical source of singlet oxygen. *Chem. Commun.* **2005**, *28*, 483–485. [CrossRef] [PubMed]
96. Wiegand, C.; Herdtweck, E.; Bach, T. Enantioselectivity in visible light-induced, singlet oxygen [2+4] cycloaddition reactions (type II photooxygenations) of 2-pyridones. *Chem. Commun.* **2012**, *48*, 10195–10197. [CrossRef] [PubMed]
97. Aubry, J.M.; Pierlot, C.; Rigaudy, J.; Schmidt, R. Reversible binding of oxygen to aromatic compounds. *Acc. Chem. Res.* **2003**, *36*, 668–675. [CrossRef]
98. Ayan, S.; Gunaydin, G.; Yesilgul-Mehmetcik, N.; Gedik, M.E.; Akkaya, E.U. Proof-of-principle for two-stage photodynamic therapy: Hypoxia triggered release of singlet oxygen. *Chem. Comm.* **2020**, *56*, 14793–14796. [CrossRef] [PubMed]
99. Zhao, X.; Liu, J.; Fan, J.; Chao, H.; Peng, X. Recent progress in photosensitizers for overcoming the challenges of photodynamic therapy: From molecular design to application. *Chem. Soc. Rev.* **2021**, *50*, 4185–4219. [CrossRef] [PubMed]
100. Huang, L.; Zhao, S.; Wu, J.; Yu, L.; Singh, N.; Yang, K.; Lan, M.; Wang, P.; Kim, J.S. Photodynamic therapy for hypoxic tumors: Advances and perspectives. *Coord. Chem. Rev.* **2021**, *438*, 213888. [CrossRef]
101. Cakmak, Y.; Kolemen, S.; Duman, S.; Dede, Y.; Dolen, Y.; Kilic, B.; Kostereli, Z.; Yildirim, L.T.; Dogan, A.L.; Guc, D.; et al. Designing excited states: Theory-guided access to efficient photosensitizers for photodynamic action. *Angew. Chem. Int. Ed. Engl.* **2011**, *50*, 11937–11941. [CrossRef]
102. Zou, J.; Yin, Z.; Ding, K.; Tang, Q.; Li, J.; Si, W.; Shao, J.; Zhang, Q.; Huang, W.; Dong, X. BODIPY Derivatives for Photodynamic Therapy: Influence of Configuration versus Heavy Atom Effect. *ACS Appl. Mater. Interfaces* **2017**, *9*, 32475–32481. [CrossRef]
103. Pang, W.; Zhang, X.F.; Zhou, J.; Yu, C.; Hao, E.; Jiao, L. Modulating the singlet oxygen generation property of meso-beta directly linked BODIPY dimers. *Chem. Commun.* **2012**, *48*, 5437–5439. [CrossRef]
104. Iyer, A.K.; Greish, K.; Seki, T.; Okazaki, S.; Fang, J.; Takeshita, K.; Maeda, H. Polymeric micelles of zinc protoporphyrin for tumor targeted delivery based on EPR effect and singlet oxygen generation. *J. Drug Target.* **2007**, *15*, 496–506. [CrossRef] [PubMed]
105. Huang, Z.; Xu, H.; Meyers, A.D.; Musani, A.I.; Wang, L.; Tagg, R.; Barqawi, A.B.; Chen, Y.K. Photodynamic therapy for treatment of solid tumors–potential and technical challenges. *Technol. Cancer Res. Treat.* **2008**, *7*, 309–320. [CrossRef] [PubMed]
106. Abels, C. Targeting of the vascular system of solid tumours by photodynamic therapy (PDT). *Photochem. Photobiol. Sci.* **2004**, *3*, 765–771. [CrossRef] [PubMed]
107. Boyle, R.W.; Dolphin, D. Structure and biodistribution relationships of photodynamic sensitizers. *Photochem. Photobiol.* **1996**, *64*, 469–485. [CrossRef]

108. Ricchelli, F. Photophysical properties of porphyrins in biological membranes. *J. Photochem. Photobiol. B* **1995**, *29*, 109–118. [CrossRef]
109. Konan, Y.N.; Gurny, R.; Allemann, E. State of the art in the delivery of photosensitizers for photodynamic therapy. *J. Photochem. Photobiol. B* **2002**, *66*, 89–106. [CrossRef]
110. Taillefer, J.; Jones, M.C.; Brasseur, N.; van Lier, J.E.; Leroux, J.-C. Preparation and characterization of pH-responsive polymeric micelles for the delivery of photosensitizing anticancer drugs. *J. Pharm. Sci.* **2000**, *89*, 52–62. [CrossRef]
111. Lu, Z.T.; Zhang, X.G.; Wu, Z.M.; Zhai, T.T.; Xue, Y.A.; Mei, L.; Li, C.X. BODIPY-based macromolecular photosensitizer with selective recognition and enhanced anticancer efficiency. *RSC Adv.* **2014**, *4*, 19495–19501. [CrossRef]
112. Khuong Mai, D.; Kang, B.; Pegarro Vales, T.; Badon, I.W.; Cho, S.; Lee, J.; Kim, E.; Kim, H.J. Synthesis and Photophysical Properties of Tumor-Targeted Water-Soluble BODIPY Photosensitizers for Photodynamic Therapy. *Molecules* **2020**, *25*, 3340. [CrossRef]
113. Liang, L.Y.; Astruc, D. The copper(I)-catalyzed alkyne-azide cycloaddition (CuAAC) "click" reaction and its applications. An overview. *Coord. Chem. Rev.* **2011**, *255*, 2933–2945. [CrossRef]
114. Kue, C.S.; Kamkaew, A.; Burgess, K.; Kiew, L.V.; Chung, L.Y.; Lee, H.B. Small Molecules for Active Targeting in Cancer. *Med. Res. Rev.* **2016**, *36*, 494–575. [CrossRef] [PubMed]
115. Wang, C.; Qian, Y. A novel BODIPY-based photosensitizer with pH-active singlet oxygen generation for photodynamic therapy in lysosomes. *Org. Biomol. Chem.* **2019**, *17*, 8001–8007. [CrossRef] [PubMed]
116. Kong, X.; Di, L.; Fan, Y.; Zhou, Z.; Feng, X.; Gai, L.; Tian, J.; Lu, H. Lysosome-targeting turn-on red/NIR BODIPY probes for imaging hypoxic cells. *Chem. Commun.* **2019**, *55*, 11567–11570. [CrossRef] [PubMed]
117. Wu, L.; Li, X.; Ling, Y.; Huang, C.; Jia, N. Morpholine Derivative-Functionalized Carbon Dots-Based Fluorescent Probe for Highly Selective Lysosomal Imaging in Living Cells. *ACS Appl. Mater. Interfaces* **2017**, *9*, 28222–28232. [CrossRef] [PubMed]
118. Zhang, Z.Q.; Yao, W.J.; Qiao, L.L.; Yang, X.; Shi, J.; Zhao, M.X. A Lysosome-Targetable Fluorescence Probe Based on L-Cysteine-Polyamine-Morpholine-Modified Quantum Dots for Imaging in Living Cells. *Int. J. Nanomed.* **2020**, *15*, 1611–1622. [CrossRef] [PubMed]
119. Li, M.L.; Tian, R.S.; Fan, J.L.; Du, J.J.; Long, S.; Peng, X.J. A lysosome-targeted BODIPY as potential NIR photosensitizer for photodynamic therapy. *Dye. Pigment.* **2017**, *147*, 99–105. [CrossRef]
120. Dost, Z.; Atilgan, S.; Akkaya, E.U. Distyryl-boradiazaindacenes: Facile synthesis of novel near IR emitting fluorophores. *Tetrahedron* **2006**, *62*, 8484–8488. [CrossRef]
121. Zhou, Y.; Cheung, Y.K.; Ma, C.; Zhao, S.; Gao, D.; Lo, P.C.; Fong, W.P.; Wong, K.S.; Ng, D.K.P. Endoplasmic Reticulum-Localized Two-Photon-Absorbing Boron Dipyrromethenes as Advanced Photosensitizers for Photodynamic Therapy. *J. Med. Chem.* **2018**, *61*, 3952–3961. [CrossRef] [PubMed]
122. Kue, C.S.; Ng, S.Y.; Voon, S.H.; Kamkaew, A.; Chung, L.Y.; Kiew, L.V.; Lee, H.B. Recent strategies to improve boron dipyrromethene (BODIPY) for photodynamic cancer therapy: An updated review. *Photochem. Photobiol. Sci.* **2018**, *17*, 1691–1708. [CrossRef]
123. Bhattacharyya, A.; Jameei, A.; Karande, A.A.; Chakravarty, A.R. BODIPY-attached zinc(II) complexes of curcumin drug for visible light assisted photo-sensitization, cellular imaging and targeted PDT. *Eur. J. Med. Chem.* **2021**, *220*, 113438. [CrossRef]
124. Singh, S.; Aggarwal, B.B. Activation of transcription factor NF-kappa B is suppressed by curcumin (diferuloylmethane) (*). *J. Biol. Chem.* **1995**, *270*, 24995–25000. [CrossRef] [PubMed]
125. Jobin, C.; Bradham, C.A.; Russo, M.P.; Juma, B.; Narula, A.S.; Brenner, D.A.; Sartor, R.B. Curcumin blocks cytokine-mediated NF-kappa B activation and proinflammatory gene expression by inhibiting inhibitory factor I-kappa B kinase activity. *J. Immunol.* **1999**, *163*, 3474–3483. [PubMed]
126. Plummer, S.M.; Holloway, K.A.; Manson, M.M.; Munks, R.J.; Kaptein, A.; Farrow, S.; Howells, L. Inhibition of cyclo-oxygenase 2 expression in colon cells by the chemopreventive agent curcumin involves inhibition of NF-kappaB activation via the NIK/IKK signalling complex. *Oncogene* **1999**, *18*, 6013–6020. [CrossRef] [PubMed]
127. Banerjee, S.; Chakravarty, A.R. Metal complexes of curcumin for cellular imaging, targeting, and photoinduced anticancer activity. *Acc. Chem. Res.* **2015**, *48*, 2075–2083. [CrossRef] [PubMed]
128. Lu, Z.T.; Mei, L.; Zhang, X.G.; Wang, Y.N.; Zhao, Y.; Li, C.X. Water-soluble BODIPY-conjugated glycopolymers as fluorescent probes for live cell imaging. *Polym. Chem.* **2013**, *4*, 5743–5750. [CrossRef]
129. Jung, E.; Shim, I.; An, J.; Ji, M.S.; Jangili, P.; Chi, S.G.; Kim, J.S. Phenylthiourea-Conjugated BODIPY as an Efficient Photosensitizer for Tyrosinase-Positive Melanoma-Targeted Photodynamic Therapy. *ACS Appl. Bio Mater.* **2021**, *4*, 2120–2127. [CrossRef] [PubMed]
130. Hossein-Nejad-Ariani, H.; Althagafi, E.; Kaur, K. Small Peptide Ligands for Targeting EGFR in Triple Negative Breast Cancer Cells. *Sci. Rep.* **2019**, *9*, 2723. [CrossRef]
131. Zhao, N.; Williams, T.M.; Zhou, Z.; Fronczek, F.R.; Sibrian-Vazquez, M.; Jois, S.D.; Vicente, M.G.H. Synthesis of BODIPY-Peptide Conjugates for Fluorescence Labeling of EGFR Overexpressing Cells. *Bioconjug. Chem.* **2017**, *28*, 1566–1579. [CrossRef]
132. Kiesslich, R.; Goetz, M.; Vieth, M.; Galle, P.R.; Neurath, M.F. Technology insight: Confocal laser endoscopy for in vivo diagnosis of colorectal cancer. *Nat. Clin. Pract. Oncol.* **2007**, *4*, 480–490. [CrossRef]
133. Ongarora, B.G.; Fontenot, K.R.; Hu, X.; Sehgal, I.; Satyanarayana-Jois, S.D.; Vicente, M.G. Phthalocyanine-peptide conjugates for epidermal growth factor receptor targeting. *J. Med. Chem.* **2012**, *55*, 3725–3738. [CrossRef]

134. Zhang, S.; Li, Y.; He, X.; Dong, S.; Huang, Y.; Li, X.; Li, Y.; Jin, C.; Zhang, Y.; Wang, Y. Photothermolysis mediated by gold nanorods modified with EGFR monoclonal antibody induces Hep-2 cells apoptosis in vitro and in vivo. *Int. J. Nanomed.* **2014**, *9*, 1931–1946. [CrossRef]
135. Kamkaew, A.; Burgess, K. Double-targeting using a TrkC ligand conjugated to dipyrrometheneboron difluoride (BODIPY) based photodynamic therapy (PDT) agent. *J. Med. Chem.* **2013**, *56*, 7608–7614. [CrossRef] [PubMed]
136. Kue, C.S.; Kamkaew, A.; Lee, H.B.; Chung, L.Y.; Kiew, L.V.; Burgess, K. Targeted PDT agent eradicates TrkC expressing tumors via photodynamic therapy (PDT). *Mol. Pharm.* **2015**, *12*, 212–222. [CrossRef] [PubMed]
137. Kue, C.S.; Kamkaew, A.; Voon, S.H.; Kiew, L.V.; Chung, L.Y.; Burgess, K.; Lee, H.B. Tropomyosin Receptor Kinase C Targeted Delivery of a Peptidomimetic Ligand-Photosensitizer Conjugate Induces Antitumor Immune Responses Following Photodynamic Therapy. *Sci. Rep.* **2016**, *6*, 37209. [CrossRef] [PubMed]
138. Radunz, S.; Wedepohl, S.; Rohr, M.; Calderon, M.; Tschiche, H.R.; Resch-Genger, U. pH-Activatable Singlet Oxygen-Generating Boron-dipyrromethenes (BODIPYs) for Photodynamic Therapy and Bioimaging. *J. Med. Chem.* **2020**, *63*, 1699–1708. [CrossRef]
139. Cao, J.J.; Zhang, M.S.; Li, X.Q.; Yang, D.C.; Xu, G.; Liu, J.Y. A glutathione-responsive photosensitizer with fluorescence resonance energy transfer characteristics for imaging-guided targeting photodynamic therapy. *Eur. J. Med. Chem.* **2020**, *193*, 112203. [CrossRef]
140. Jiang, X.J.; Lau, J.T.; Wang, Q.; Ng, D.K.; Lo, P.C. pH- and Thiol-Responsive BODIPY-Based Photosensitizers for Targeted Photodynamic Therapy. *Chemistry* **2016**, *22*, 8273–8281. [CrossRef]